The Canadian Mineralogist
Vol. 37, pp. 1343-1362(1999)

LUDWIGITE FROM THE TYPE LOCALITY, OCNA DE FIER, ROMANIA: NEW DATA AND REVIEW

STEFAN MARINCEA[§]

Department of Mineralogy, Geological Institute of Romania, 1 Caransebes Str., RO-78344, Bucharest, Romania

ABSTRACT

Ludwigite from the type locality, Ocna de Fier, Banat, Romania, was re-investigated in order to establish undocumented chemical and physical properties. The mineral occurs in boron-bearing magnesian skarns, in a restricted association that includes calcite, forsterite (fayalite 0.92–2.60%, tephroite 0.75–1.26%), magnetite (magnesioferrite 18.48–46.31%) and clinohumite (X_{Fe} = 0.59%, X_F = 40.91%). The host skarns are developed at the contact between an intrusive Upper Cretaceous "banatitic" body, which is mainly granodioritic, and metasomatized Mesozoic limestones. Ludwigite from Ocna de Fier is closer to the magnesian end-member than previously reported. The analyzed samples are compositionally variable, with vonsenite ranging from 4.41 to 14.27 mol.%, minor azoproite [up to 0.10 mol.% $(Mg,Fe^{2+})_2(Ti^{4+},Mg)(BO_3)O_2$], and less than 6.55 mol.% $(Mg,Fe^{2+})_2Al(BO_3)O_2$ in solid solution, and with minor Sn, Sb, Cr, Ni, Co, Mn and Zn. Cell parameters [*a* 9.225(8) – 9.290(6), *b* 12.233(9) – 12.334(6), *c* 3.033(4) – 3.057(3) Å] are influenced by both Fe^{2+} and Al contents. The mean reflectance is approximately 11%, and the mean index of refraction is 1.95. A strong magnetic anisotropy is observed; the maximum of susceptibility (12511.76•10^6 e.m.u.) was measured along a direction coincident with fiber elongation. The Mössbauer spectroscopy indicates the superparamagnetic behavior of the mineral. The splitting of internal vibrational modes of BO_3 group in the infrared spectra is consistent with a C_{3v} or C_s point symmetry of the BO_3 group, which is characteristic of magnesian ludwigite. Heated in air, the mineral is stable up to 1000°C. The compositional data, combined with information on the experimental synthesis of borates, indicate a temperature of crystallization at 600–650°C and oxygen fugacities of 10^{-18} – 10^{-14} atm.

Keywords: ludwigite, magnesian skarns, X-ray data, thermal behavior, magnetic behavior, Mössbauer spectroscopy, infrared-absorption data, crystal chemistry, Ocna de Fier, Romania.

SOMMAIRE

Une nouvelle étude de la ludwigite provenant de la localité-type, Ocna de Fier, Banat, en Roumanie, a été entreprise pour mettre en évidence quelques caractères chimiques et physiques ignorés jusqu'à présent. Le minéral apparaît dans des skarns magnésiens minéralisés en bore; il fait partie d'un assemblage restreint, à calcite, forstérite (fayalite 0.92–2.60%, téphroïte 0.75–1.26%), magnétite (magnésioferrite 18.48–46.31%) et clinohumite (X_{Fe} = 0.59%, X_F = 40.91%). Les skarns hôtes sont développés au contact d'un massif intrusif d'âge Crétacé supérieur, de composition granodioritique ("banatitique"), avec des calcaires métasomatisés d'âge mésozoïque. La ludwigite de Ocna de Fier est plus proche du pôle magnésien qu'on a prétendu antérieurement. Les échantillons analysés ont une composition variable, avec une proportion du composant vonsénite entre 4.41 et 14.27% (base molaire), peu d'azoproïte (jusqu'à 0.10% de $(Mg,Fe^{2+})_2(Ti^{4+},Mg)(BO_3)O_2$), et jusqu'à 6.55% de $(Mg,Fe)_2Al(BO_3)O_2$ dans la solution solide, et contiennent des teneurs mineures en Sn, Sb, Cr, Ni, Co, Mn et Zn. Les paramètres de la maille réticulaire [*a* 9.225(8) – 9.290(6), *b* 12.233(9) – 12.334(6), *c* 3.033(4) – 3.057(3) Å] sont influencés également par les teneurs en Fe^{2+} et Al. Le pouvoir réflecteur moyen se situe autour 11%, et l'indice moyen de réfraction, autour de 1.95. Une puissante anisotropie magnétique peut être mise en évidence; une valeur maximale de susceptibilité (12511.76•10^6 u.e.m.) a été mesurée le long de l'allongement des fibres. La spectroscopie de Mössbauer montre un comportement superparamagnétique du minéral. La dégénérescence des modes internes de vibration du groupe BO_3 dans les spectres infrarouges est compatible avec une symétrie ponctuelle C_{3v} ou C_s de ce groupe, ce qui est caractéristique de la ludwigite magnésienne. Chauffé dans l'air, le minéral est stable jusqu'à 1000°C. Les données de composition, combinées avec celles issues des synthèses expérimentales des borates, indiquent des températures de cristallisation de 600–650°C pour des fugacités d'oxygène de 10^{-18} – 10^{-14} atm.

Mots-clés: ludwigite, skarns magnésiens, données de diffraction X, analyse thermique, comportement magnétique, spectroscopie de Mössbauer, spectrométrie d'absorption infrarouge, chimie cristalline, Ocna de Fier, Roumanie.

[§] *E-mail address*: marincea@ns.igr.ro

INTRODUCTION

Ludwigite is a quite widespread oxyborate mineral with an extended general formula of $(Mg,Fe^{2+},Mn^{2+},Ni)_2(Fe^{3+},Al,Ti,Sb^{5+},Sn^{4+},Cr^{3+},Mn^{3+},Mg)(BO_3)O_2$ type. It was first described by Tschermak (1874) from Ocna de Fier, Banat, Romania, formerly known as Moravicza, Vaskö or Eisenstein. Tschermak (1874) gave the first chemical and optical data on the new mineral, and Mallard (1887) provided crystallographic data.

In subsequent studies of ludwigite, authors made use of material from the type locality to compare it with ludwigite from several other occurrences, resulting in additional chemical (Schaller 1911), optical (Larsen 1921, Capdecomme 1946), X-ray (Shabynin 1955), infrared (Aleksandrov *et al.* 1965) and structural data (Bonazzi & Menchetti 1989) on ludwigite from Ocna de Fier. Two monographic studies carried out by Codarcea *et al.* (1957) and Koch (1960) provided valuable information concerning its composition, optical properties and mineral associations, and a broader study by Kissling (1967) added new morphological, optical, thermal (DTA), chemical and diffractometric data, and a detailed paragenetic analysis.

In order to complement the existing data, a detailed study was undertaken using reflectance, electron microprobe, inductively coupled plasma – atomic emission spectrometry (ICP–AES), inductively coupled plasma – mass spectrometry (ICP–MS), X-ray diffraction, susceptibility, Mössbauer, thermal and infrared absorption analyses. The new data are important in view of the widespread occurrences of ludwigite in magnesian skarn deposits (Aleksandrov 1982, Pertsev 1991).

GEOLOGICAL SETTING

As described by Kissling (1967), ludwigite at Ocna de Fier occurs as lenses hosted by the dolomitic marble developed in the outer zone of a skarn complex located in the western part of the South Carpathians, approximately 12 km northwest of Resita, the major city in the area. A pronounced zonation of the ludwigite-bearing lenses shows that these are in fact small metasomatic bodies consisting of an assemblage of ludwigite, magnetite, forsterite, clinohumite and products of their alteration.

Both skarn and marble are developed in the contact area of an intrusive body named "the Ocna de Fier – Dognecea granodioritic pluton" by Russo-Sandulescu *et al.* (1986). This body is generally considered to represent a southward continuation of the Bocsa massif, a major composite pluton of Upper Cretaceous age (Russo-Sandulescu *et al.* 1986). In general, such magmatic bodies are described by the collective term "banatite", after von Cotta (1864), who first described at the *locus tipicus*, Banat, a consanguineous series of compositionally intermediate intrusive rocks of Late Cretaceous – Paleogene age. The Ocna de Fier – Dognecea body seems to have been emplaced at a relatively shallow depth, during the third phase of intrusion of the calc-alkaline magmas in the area (Bocsa 3 according to Russo-Sandulescu *et al.* 1986). U–Pb radiometric analyses on zircon indicate 79.6 ± 2.5 Ma for the Bocsa 3 phase, whereas the Ocna de Fier granitic rocks yield U–Pb zircon ages of 75.5 ± 1.6 Ma (Nicolescu 1998), indicating that the two magmatic bodies may be coeval. The intrusive body at Ocna de Fier consists mainly of granodiorite and granodiorite porphyry with subordinate quartz monzodiorite and melanocratic diorite (Russo-Sandulescu *et al.* 1986).

Skarns from Ocna de Fier occupy extensive zones within the contact area. Their protolith consisted of micritic limestones with intraclastic levels and calcareous sandstones of Upper Jurassic – Lower Cretaceous age, deposited in the Ezeris – Cârnecea zone of sedimentation. They form discontinuous bands, irregular or tabular bodies and metasomatic veins, and display an obvious metasomatic zoning, essentially exhibiting an inner Ca-rich skarn zone with mainly andraditic garnet, and an outer zone with Mg-rich skarns, developed near the dolomitized marble. Cioflica & Vlad (1973) described these features as typical of the Ocna de Fier "skarn type".

The magnesium-rich skarns are mainly diopside- or tremolite-rich, with lesser amounts of phlogopite and subordinate forsterite and clinohumite; the latter are generally serpentinized. Dolomitized marbles hosting ludwigite are invariably adjacent to this type of skarn, being separated from them by a thin zone of serpentine. Spatially they are disposed around Danilii Hill, between Terezia quarry (in the north) and Iuliana quarry (in the south; Fig. 1). The most important occurrences of ludwigite are those in Magnet, Arhangheli, Iuliana, Terezia and Delius quarries, as well as in some old mines, *e.g.*, Jupiter and Reichenstein (Kissling 1967). Only the first four sites of mining activity are still accessible. The *locus tipicus* for the mineral approximately corresponds to an old pit that was removed during the exploitation of the Magnet quarry.

ANALYTICAL METHODS

A brief description of the main analytical methods used during this study is given below. More detailed information about methods of sample preparation and analytical techniques is available in Marincea (1998).

Electron-microprobe analyses were performed in wavelength-dispersion mode, on standard polished thin sections. The apparatus used was a CAMECA SX–50 electron microprobe set at an accelerating voltage of 15 kV (except 5 kV for B), a beam current of 10 nA, and a beam diameter of 5 μm (10 μm for B, on separate spots). Natural diopside (Si, Mg and Ca$K\alpha$), synthetic hematite (Fe$K\alpha$), natural orthoclase (K and Al$K\alpha$), natural pyrophanite (Ti and Mn$K\alpha$), synthetic fluorine (F$K\alpha$) and boron nitride (B$K\alpha$) were used as standards.

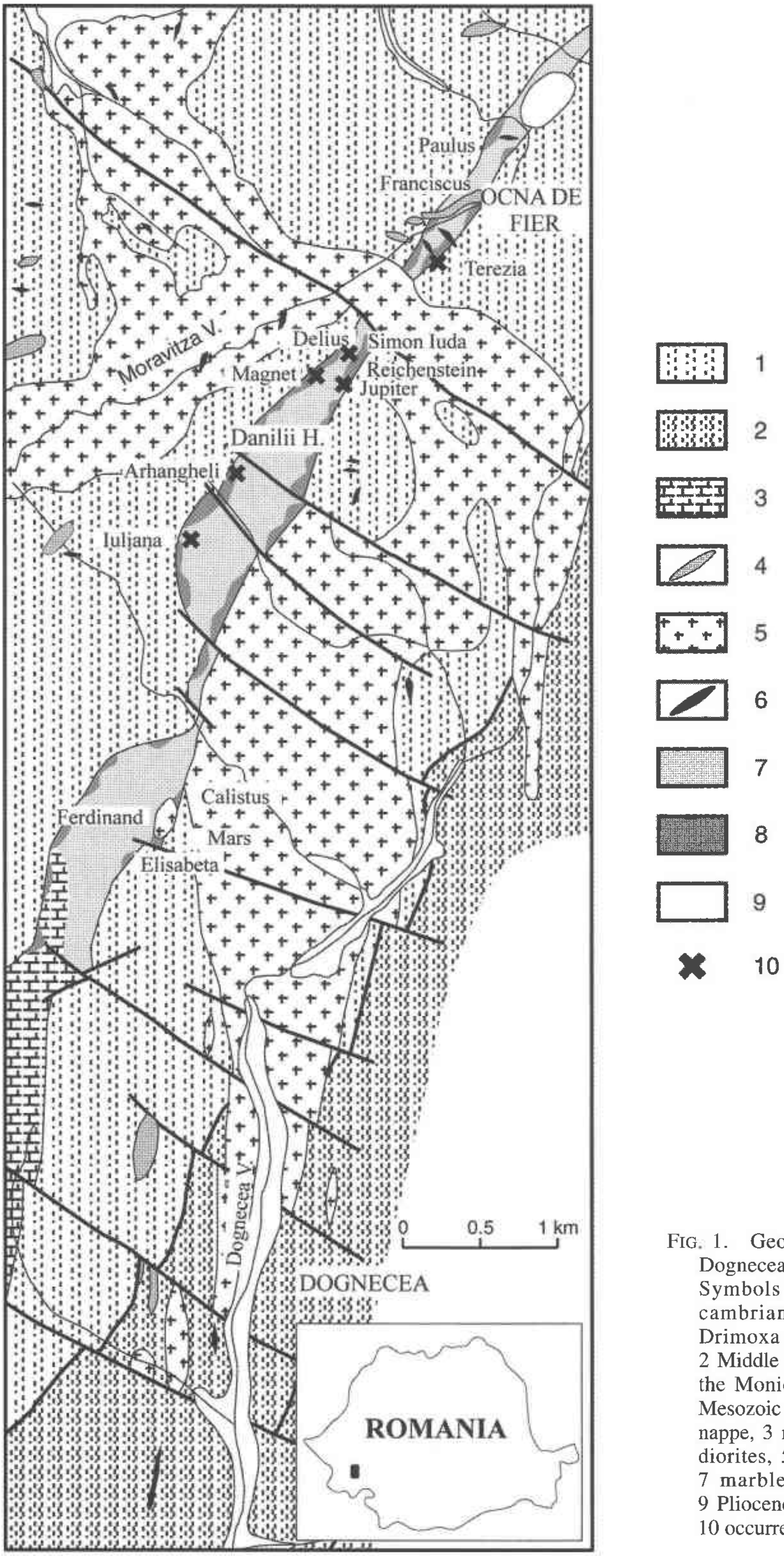

FIG. 1. Geological sketch of Ocna de Fier – Dognecea area (redrawn from Ilinca 1998). Symbols in the legend represent: 1 Precambrian metamorphic rocks (Bocsita–Drimoxa Formation) in the Bocsa nappe, 2 Middle Paleozoic metamorphosed rocks in the Moniom nappe and Upper Paleozoic – Mesozoic sedimentary formations in the Resita nappe, 3 marble, 4–6 "banatites" (4 gabbro–diorites, 5 granodiorites, 6 lamprophyres), 7 marble and hornfels, 8 skarn bodies, 9 Pliocene – Quaternary sedimentary cover, 10 occurrences of ludwigite.

Counting time was 20 s per element. Data reduction was done using the PAP correction procedure (Pouchou & Pichoir 1985). The scanning electron microscopy study (SEM) was performed separately, using a JEOL JSM–840 apparatus set at an acceleration voltage of 15 kV and a beam current of 10 nA.

Wet-chemical analyses of ludwigite samples from Ocna de Fier were done after a careful separation, which used the technique recommended by Vlisidis & Schaller (1974). Carefully hand-picked and pulverized material was first etched with cold 1:3 nitric acid, then purified using both the Franz magnetic separator and heavy liquids in separatory funnels. Prior to analysis, separates of ludwigite were decomposed by melting with Na_2CO_3 in nickel crucibles, then removed with water. Except for boron, whose concentration was determined by inductively coupled plasma – atomic emission spectrometry, the concentration of the cations was determined by standard methods of quantitative analysis (gravimetry, colorimetry and absorption spectrometry) following techniques recommended by Maxwell (1968) and Iosof & Neacsu (1980). The Penfield method was used for water determinations.

The values of reflectance were measured using an Opton Microphotometer equipped with a HTV photomultiplier and an MSP–21 analogous digital converter. Conditions used were: 25 W at 6 V as power supply for the source (a WFG illuminator), 50× magnification and 0.8 numerical aperture for the objective, lamp aperture of 0.5, 60 μm diameter for the diaphragm. The measurements were made against a SiC reflectance standard.

Mössbauer spectra of ludwigite samples were obtained using a constant acceleration, mechanically driven, Mössbauer spectrometer. The spectra were taken with a ^{57}Co rhodium-matrix source (with initial activity of 5 mCi), with both source and absorber at room temperature (22°C). Data were accumulated in 512 channels, which covered the Doppler velocity range of ±15.0 mm/s. The spectra were fitted by least-squares method assuming Lorentzian lines, and the velocity scale was normalized with respect to the center of the spectrum of metallic iron at room temperature.

X-ray powder-diffraction patterns were obtained using an automated Siemens D–5000 Krystalloflex diffractometer, with graphite-monochromatized Cu$K\alpha$ radiation (λ = 1.54056 Å), at 40 kV and 30 mA. The data were collected over the 2θ range 5–90°, using a step size of 0.04°2θ and a 2 s counting time at each step. Synthetic spinel (a = 8.0835 Å) was used as an internal standard.

Thermal curves were drawn using a MOM 1500 D derivatograph used with a Pt – PtRh thermocouple. They were obtained by heating the sample at 10°C/min. in the range 20° to 1000°C, with a continuous air supply of 50 mL/min. Because the danger of iron diffusing into platinum at low fugacities of oxygen (Larson & Chipman 1954), followed by the destruction of the apparatus, the heating was stopped before the fusion of ludwigite. The material used for analysis was separated from the powders used for chemical analysis, after conventional magnetic and heavy-liquid separation, but before chemical treatment.

The infrared absorption spectra were obtained using a SPECORD M–80 spectrometer and a standard pressed disk technique. Samples were prepared by diluting the ludwigite powders in KBr, in ratios of about 1:500, and compacting under 2500 N/cm^2 pressure.

ASSOCIATED MINERALS

Results of an extensive analysis of the associated minerals, including the carbonate phases, was given by Marincea (1998). The list of these minerals, restricted to the species occurring in the ludwigite-bearing zones, includes magnetite, forsterite, clinohumite, szaibelyite, calcite, dolomite, ankerite, antigorite, lizardite, clinochlore, pyroaurite, goethite, lepidocrocite, pyrite, pyrrhotite, arsenopyrite, chalcopyrite, sphalerite, galena, marcasite and covellite. Because only the first three minerals show paragenetic relations with ludwigite, and because szaibelyite and the serpentines occur by direct alteration of primary minerals, only these species will be investigated below.

Magnetite is the only spinel phase found in the samples investigated. Franklinite, mentioned by Koch (1960), was not found in any of them. At Ocna de Fier, magnetite may occur as monomineralic bands of optically unzoned grains or as isolated grains interstitial to silicates (*i.e.*, forsterite, clinohumite) or to ludwigite. The cell parameter calculated for three different samples by least squares, using 13–14 X-ray powder reflections in the 2θ range of 10 to 100°, varies between 8.388(4) and 8.400(2) Å. These values are close to that given by Basta (1957) for stoichiometric magnetite (a = 8.396 Å). Paragenetic relations between borates and the spinel indicate two generations of magnetite, in equilibrium with ludwigite and szaibelyite, respectively. It is to be expected that magnetite I, which cocrystallized with ludwigite, will have higher contents of Mg than magnetite II, which replaces ludwigite and cocrystallized with szaibelyite, because the magnesium is preferentially fixed by szaibelyite. Results of electron-microprobe analyses (Table 1) confirm this hypothesis. The magnetite does exhibit a bimodal distribution with respect to its Mg content: between 18.48 and 46.31 mol.% magnesioferrite may be deduced in magnetite I, as compared to 11.23 mol.% in the only analyzed sample of magnetite II. The magnetite grains belonging to the same generation are remarkably homogeneous within the limits of the same crystal and of the same sample. This level of homogeneity represents a characteristic feature of all the analyzed phases, including oxides, silicates and borates. Consequently, the results presented in Table 1 are representative of crystals in the same thin

TABLE 1. RESULTS OF ELECTRON-MICROPROBE ANALYSES OF SELECTED SAMPLES OF MAGNETITE ASSOCIATED WITH LUDWIGITE*

SAMPLE	1168	1799	1867	1975	2073	2218	2219	2221	1168
TYPE	mgt I	mgt I	mgt I	mgt I	mgt I	mgt I	mgt I	mgt I	mgt II
No.(1)	7	3	5	3	4	4	5	8	3
TiO_2	0.010	0.015	0.016	0.028	0.000	0.044	0.071	0.027	0.030
Al_2O_3	0.047	0.005	0.154	0.017	0.301	0.068	0.079	0.024	0.045
Fe_2O_3(2)	71.218	70.729	71.518	72.256	70.786	73.466	71.122	71.326	69.950
FeO(2)	23.767	25.272	21.742	20.069	24.547	16.911	23.872	23.257	27.315
MnO	0.605	0.642	1.467	1.410	0.318	0.833	0.444	0.846	0.593
MgO	4.259	3.298	5.080	6.190	3.998	8.591	4.400	4.491	1.981
CaO	0.094	0.039	0.023	0.030	0.050	0.087	0.012	0.029	0.086
TOTAL(3)	100.00	100.00	100.00	100.00	100.00	100.00	100.00	100.00	100.00
NUMBER OF IONS ON THE BASIS OF 24 CATIONS									
Ti	0.002	0.003	0.003	0.006	0.000	0.010	0.016	0.006	0.007
Al	0.016	0.002	0.054	0.006	0.106	0.023	0.028	0.008	0.016
Fe^{3+}	15.980	15.992	15.940	15.983	15.894	15.957	15.940	15.980	15.970
Fe^{2+}	5.926	6.350	5.385	4.933	6.126	4.082	5.946	5.791	6.931
Mn	0.153	0.163	0.368	0.351	0.080	0.204	0.112	0.213	0.152
Mg	1.893	1.477	2.243	2.712	1.778	3.697	1.954	1.993	0.896
Ca	0.030	0.013	0.007	0.009	0.016	0.027	0.004	0.009	0.028

* Results expressed in wt.%

(1) number of point analyses

(2) as deduced from FeO_T, after the adjustment of the ferric/ferrous ratios in order to fulfill the charge balance

(3) totals recalculated to 100 %

TABLE 2. RESULTS OF REPRESENTATIVE ELECTRON-MICROPROBE ANALYSES OF SILICATES ASSOCIATED WITH LUDWIGITE*

Sample	1168	1891	2073	2218	2219	1873	1866	2218	1975
Mineral	Fo(5)	Fo(5)	Fo(5)	Fo(5)	Fo(5)	Chu(5)	Lz(5)	Lz(5)	Atg(5)
No.(1)	4	3	3	5	6	5	3	5	2
SiO_2	42.056	42.241	43.222	42.554	42.094	37.436	38.401	38.335	41.291
TiO_2	n.d.	0.001	0.083	0.040	0.014	0.079	n.d.	n.d.	n.d.
Al_2O_3	0.017	n.d.	0.011	n.d.	n.d.	n.d.	3.195	1.644	1.534
B_2O_3	n.a.	n.a.	n.a.	n.a.	n.a.	n.d.	n.d.	1.253	n.d.
MgO	54.539	55.298	54.931	54.400	55.449	55.579	38.517	39.304	37.704
FeO(2)	2.596	1.169	0.906	1.753	1.478	0.586	2.895	2.637	3.205
MnO	0.767	1.190	0.833	1.233	0.929	0.296	0.093	0.090	0.061
CaO	0.025	0.101	0.014	0.020	0.036	0.032	0.015	0.022	0.193
F	n.a.	n.a.	n.a.	n.a.	n.a.	2.467	n.d.	n.d.	n.d.
H_2O(3)	n.a.	n.a.	n.a.	n.a.	n.a.	1.688	n.c.	n.c.	n.c.
Total	100.00	100.00	100.00	100.00	100.00	98.163	83.116	83.285	83.988
NUMBER OF IONS ON THE BASIS OF N(4) OXYGEN ATOMS									
Si	1.000	1.000	1.018	1.008	0.997	4.017	3.776	3.734	4.002
Ti	0.000	0.000	0.001	0.001	0.000	0.006	-	-	-
Al	0.000	0.000	0.000	0.000	0.000	0.000	0.370	0.189	0.175
B	-	-	-	-	-	0.000	0.000	0.211	0.000
Mg	1.932	1.950	1.927	1.921	1.957	8.893	5.646	5.708	5.448
Fe^{2+}	0.052	0.023	0.018	0.035	0.029	0.053	0.238	0.215	0.260
Mn	0.015	0.024	0.017	0.025	0.019	0.027	0.008	0.007	0.005
Ca	0.001	0.003	0.000	0.001	0.001	0.004	0.002	0.002	0.020
F^-	-	-	-	-	-	0.837	-	-	-
$(OH)^-$	-	-	-	-	-	1.209	n.c.	n.c.	n.c.

* Results expressed in wt.%

(1) number of point analyses

(2) all Fe was considered in divalent state of oxidation

(3) as calculated in order to fulfill the charge balance

(4) 4 (O) for forsterite, 16 (O) and 13 cations for clinohumite, 14 (O) for serpentines.

(5) Fo: forsterite, Chu: clinohumite, Lz: lizardite, Atg: antigorite.

Other abbreviations: n.a.: not analyzed; n.c.: not calculated; n.d.: not detected

section. A late-stage partial alteration of both generations of magnetite produced goethite and lepidocrocite, which may occur on fractures and fill cavities in the masses of magnetite.

Forsterite was identified in almost all the analyzed samples. It occurs as disseminated crystals or, more commonly, in irregular aggregates of euhedral or subhedral crystals, enclosed by the massive ludwigite and partially serpentinized. Optically, the mineral is biaxial positive with a very high $2V$ angle ($86 < 2V < 88°$), which indicates a high forsterite content (Tröger 1969). The high forsterite content is also supported by the X-ray powder-diffraction data. On the basis of the position of the (130) spacing [d(130) in the range 2.764 to 2.767 Å] and using the relation proposed by Schwab & Kustner (1977):

$$\text{Fo (mol.\%)} = 100 - [7.522 - 14.907\,(3.020 - d\,(130))^{1/2}]\bullet 100\ (\%)$$

all the investigated samples contain between 97.5 and 100.0 mol.% forsterite.

Results of electron-microprobe analyses of representative magnesian silicates associated with ludwigite (Table 2) confirm that forsterite from Ocna de Fier has a low content of Fe and Mn: between 0.92 and 2.60 mol.% fayalite, and between 0.75 and 1.26 mol.% tephroite are indicated.

Clinohumite in the borate-bearing skarns occurs most commonly as discrete subhedral to euhedral grains in the matrix of ludwigite and magnetite, but it is also found as clusters of crystals where it coexists with forsterite. Normally, the crystals are polysynthetically twinned on (001). The mineral is biaxial positive, with $71 < 2V < 78°$ and extinction angles $c{:}\alpha$ in the range 9–11°. The weak pleochroism (colorless along γ and β, light yellow along α) and the relatively low birefringence are consistent with the chemical data in Table 2, which indicate an iron-poor [$X_{Fe} = 100\bullet Fe^{2+}/(Fe^{2+} + Mg) = 0.59$] hydroxyl-clinohumite [$X_F = 100\bullet F/(F + OH) = 40.91$].

Lizardite typically occurs as a rim on forsterite or clinohumite or, more commonly, in pseudomorphic mesh-textures after forsterite. Non-pseudomorphic textures of interpenetrating type occur rarely and consist of *antigorite* (identified on the basis of X-ray powder data, using the scheme of Whittaker & Zussman 1956). All the pseudomorphic textures have mesh-centers of forsterite or "serpophite" (lizardite-1*T* according to Wicks & Zussman 1975). Optically, the mesh-rims have negative elongation, which characterizes an α-serpentine *sensu* Wicks & Zussman (1975). Taking into account that the α-mesh-rims consist mainly of lizardite-1*T* (Wicks & Zussman 1975, Wicks & Whittaker 1977, Cressey 1979), lizardite is inferred to be present in all the samples examined. This inference is supported by the X-ray powder-diffraction study, because all of the analyzed samples behave as lizardite according to the criteria of Whittaker & Zussman (1956): they show a high-intensity line at a d value of 2.499–2.503 Å and a strong pair of lines at 1.501–1.503 Å and 1.534–1.537 Å, whereas the strong line of antigorite around 1.563 Å is absent. Note that the chemical differences between lizardite and antigorite (Table 2) obey the trend pointed out by Whittaker & Wicks (1970).

Szaibelyite occurs as bunches of small needle-like crystals, near the limits of optical resolution. It forms polycrystalline pseudomorphs after ludwigite, being generally intergrown with strings of magnetite II. The average unit-cell parameters, deduced by least-squares refinement of three sets of X-ray powder data, are *a*

TABLE 3. RESULTS OF ELECTRON-MICROPROBE ANALYSES OF SELECTED SAMPLES OF SZAIBELYITE

Sample	1167	1168	1415	1799	1866
No.(1)	10	10	3	4	6
B_2O_3	41.008	41.101	42.096	41.444	41.226
Al_2O_3	0.111	0.074	0.019	0.301	0.034
MgO	46.976	46.919	46.457	45.374	46.903
MnO	0.336	0.362	0.302	0.253	0.315
FeO(2)	0.847	0.815	0.573	2.080	0.852
CaO	0.029	0.039	0.022	0.029	0.016
H_2O(3)	10.792	10.666	9.722	10.071	10.570
F	0.040	0.067	0.058	0.049	0.025
Total	100.139	100.043	99.249	99.601	99.941
NUMBER OF IONS ON THE BASIS OF 2 B AND 4 O					
B	2.000	2.000	2.000	2.000	2.000
Al	0.004	0.002	0.001	0.010	0.001
Mg	1.978	1.972	1.906	1.891	1.965
Mn	0.008	0.009	0.007	0.006	0.008
Fe^{2+}	0.020	0.019	0.013	0.049	0.020
Ca	0.001	0.001	0.001	0.001	0.000
$(OH)^-$	2.022	2.002	1.852	1.920	1.987
F^-	0.004	0.006	0.005	0.004	0.002
COMPOSITION IN END-MEMBERS (MOL.%)					
szaibelyite	98.55	98.55	98.91	97.12	98.60
sussexite	0.40	0.45	0.36	0.31	0.40
$Fe^{2+}_2(B_2O_4OH)(OH)$	1.00	0.95	0.68	2.52	1.00
"sibirskite"	0.05	0.05	0.05	0.05	0.00

(1) number of point analyses.
(2) total iron as FeO.
(3) as calculated in order to fulfill the charge balance.

12.545(4), *b* 10.388(9), *c* 3.135(8) Å, β 95.68(27)°. Results of electron- microprobe analyses (Table 3) show that the szaibelyite is poor in Mn + Fe and contains as usual a very low content of Ca. Up to 0.45 mol.% sussexite (the Mn end-member) and 2.52 mol.% $Fe_2(B_2O_4OH)(OH)$ may be deduced, and the "sibirskite" component amounts to 0.05 mol.%. It is worth noting that the ferrous component is always greater than the manganoan one, a feature that appears to characterize all the szaibelyite pseudomorphs after ludwigite in the Romanian deposits (Marincea 1998).

MORPHOLOGY OF THE CRYSTALS

At Ocna de Fier, ludwigite generally occurs as irregular bands of randomly oriented crystals. These bands ("Liesegang bands" according to Kissling 1967), 3 to 20 cm wide, predominantly consist of ludwigite and alternate with magnetite bands having approximately the same thickness. They exhibit a texture that obviously results from a metasomatic process. Occasionally, ludwigite aggregates occur as nests or veins, usually enclosed by the magnetite mass. Generally, ludwigite in these aggregates forms fibrous masses with a silky luster and pitch-black to olive-black color. The component crystals are fibrous and form parallel, radiating or interwoven aggregates, which give to the mass a felt-like appearance. Coarser radiating or fan-like aggregates are scarce; they contain bunches of crystals of up to 35 mm long (reported up to 60 mm by Koch 1960) and up to 2 mm thick.

The SEM study shows that the individual crystals have a restricted number of forms. Prisms {*hk*0} are identified as {110} and {120}. No terminal faces can be distinguished. The frequency of subparallel and parallel intergrowths makes a complete morphological study difficult.

The SEM and reflected-light studies document a curved appearance of some bunches of ludwigite crystals. The individual crystals that compose these aggregates are commonly truncated by narrow fractures, oriented perpendicular to [001]. Fractures of this kind may be observed in Figure 2A. This system of fractures, locally filled with szaibelyite and secondary magnetite (Fig. 2B), progressively changes the orientation of bunches of ludwigite crystals, which appear curved. The extensive system of longitudinal fractures, called "separation lines" by Koch (1960) and always filled by magnetite and szaibelyite, are considered to be the result of the unequal expansion in volume caused by the formation of szaibelyite.

OPTICAL AND PHYSICAL PROPERTIES

The study of thin sections emphasizes the practically opaque nature of ludwigite from Ocna de Fier. Only some fine needle-like crystals have a translucent rim, visible where they are embedded in the carbonate mass; in these cases, the mineral shows a weak pleochroism in dark brown to reddish brown shades. The directions of vibration cannot be specified, but may be inferred by comparison with the data in the literature (*i.e.*, Capdecomme 1946, Leonard *et al.* 1962), which specify that the dark colors correspond to γ. This behavior is consistent with a low Al content of a magnesian member of the ludwigite – vonsenite series. The indices of refraction of sample 1168, measured in immersion and by comparison with standard Sovirel glasses, using oblique illumination and sodium light (λ = 589 nm) are γ 2.03(2) and β (= α) 1.90(2). These values are in good

TABLE 4. PHYSICAL PARAMETERS OF SELECTED SAMPLES OF LUDWIGITE FROM OCNA DE FIER

Sample	$M^{(1)}$	$V^{(2)}$	D_x	K_C	$D'_x{}^{(3)}$	$\bar{n}_x{}^{(4)}$	$K_P{}^{(5)}$	$1-(K_P/K_C)$
1167	197.832*	345.537	3.801	0.2528	3.730	1.961	0.2482	0.018
1168	198.607*	347.078	3.780	0.2516	3.748	1.951	0.2495	0.008
1168	204.219•	347.078	3.906	0.2507	3.761	1.979	0.2414	0.037
1415	199.393•	346.670	3.819	0.2498	3.775	1.954	0.2470	0.011
1417	197.672*	346.448	3.789	0.2521	3.740	1.955	0.2490	0.012
1418	197.924*	345.780	3.789	0.2516	3.748	1.953	0.2490	0.010
1439	200.534*	346.664	3.841	0.2509	3.758	1.964	0.2456	0.021
1439	199.911•	346.664	3.829	0.2498	3.775	1.956	0.2463	0.014
1798	198.530*	346.188	3.808	0.2510	3.757	1.956	0.2477	0.013
1799	199.209•	346.927	3.813	0.2523	3.738	1.962	0.2474	0.019
1866	197.942•	346.281	3.796	0.2503	3.767	1.950	0.2485	0.007
1867	198.795•	346.345	3.811	0.2485	3.795	1.947	0.2475	0.004
2218	200.478•	346.435	3.842	0.2525	3.735	1.970	0.2455	0.028

(1) molecular mass; * as calculated on the basis of wet-chemical analyses; • as calculated on the basis of electron-microprobe analyses.
(2) unit-cell volume (in Å^3), as deduced from least-squares refinement of X-ray powder data.
(3) calculated according to Gladstone-Dale law, by using the mean index of refraction ($\bar{n}$ = 1.943), and the chemical molar refractivity (K_C).
(4) $\bar{n}_x = D_x \cdot K_C + 1$.
(5) $K_P = (\bar{n} - 1)/D_x$.

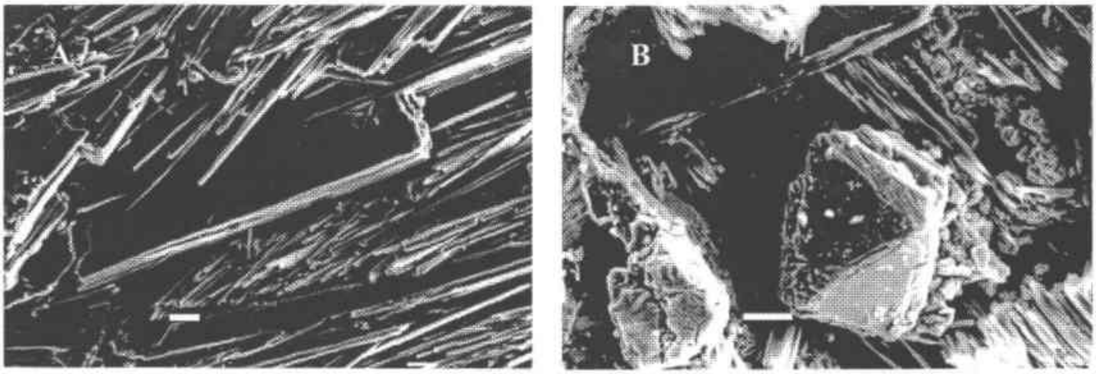

FIG. 2. Scanning electron micrographs showing truncated crystals of ludwigite in a felt-like aggregate (A) and a magnetite octahedron disposed on a fissure in ludwigite (B). Scale bar = 10 μm.

agreement with those reported by Palache *et al.* (1951) for ludwigite from the type locality: γ 2.02(2) and β (= α) 1.85(1). Data in Table 4 show that the mean indices of refraction, calculated according to the Gladstone–Dale rule using the calculated densities and the molar refractivities (K_C) derived from chemical compositions, fit well with the resulting mean index of refraction [$\bar{n} = (\alpha + \beta + \gamma)/3 = 1.943$].

Polished sections show that, in plane-polarized light, ludwigite from Ocna de Fier is distinctly bireflectant in pinkish gray (|| *Z*) to dark greenish gray (⊥ *Z*) tints. Under crossed nicols, it shows a strong anisotropy in yellowish brown (|| *Z*) to bluish violet gray (⊥ *Z*) colors. No internal reflections were observed.

The minimum ($R_{\min}$) and the maximum ($R_{\max}$) values of reflectance were measured in air, at wavelengths of 498, 553, 590 and 650 nm, in sections of maximum anisotropy because of the difficulty in obtaining oriented sections, for two different samples. The observed values are listed in Table 5, whereas the reflectance curves drawn for one of the samples are given in Figure 3. Each value in Table 5 represents an average of 1000 measurements. The mean reflectance values are generally higher than those reported by Uytenbogaardt & Burke (1971) (*R* in the range 8–10%), but closely approximate the 10% value. In fact, these values are similar to those documented in some other examples of ludwigite by Strona (1964) (*R* = 9.4 %) or Leonard *et al.* (1962) (*R* in the range 9.5–11.4%).

On the basis of the measured values of reflectance, a calculation of the indices of refraction may be attempted, using the Fresnel equation in the form that assumes an absorption coefficient *k* = 0. The translucency of some crystal rims suggests that *k* may be neglected; it results that $n \cong (1 + R \pm 2\sqrt{R}) / (1 - R)$. The indices of refraction that were obtained are listed in Table 5. The mean values ($n_{\min}$ in the range 1.74–1.83,

TABLE 5. OPTICAL PARAMETERS OF SELECTED SAMPLES OF LUDWIGITE FROM OCNA DE FIER

1. SAMPLE 1167 (IULIANA QUARRY)

Wavelength (nm)		488	553	590	650	Mean
Acceleration voltage (V)		791	795	802	756	
Reflectance	$R_{\min}$	11.32(12)	10.56(9)	9.83(11)	9.35(12)	10.27
	$R_{\max}$	14.96(13)	13.79(12)	13.12(11)	13.01(10)	13.72
	R_{mean}	13.14	12.18	11.47	11.18	11.99
$\Delta R = R_{\max} - R_{\min}$		3.64	3.23	3.29	3.66	3.46
Bireflectance (Δ R %)		27.70	26.52	28.68	32.74	28.86
Indices of refraction	$n_{\max}$	1.85	1.89	1.94	1.97	1.91
	$n_{\min}$	1.70	1.74	1.76	1.77	1.74
	n_{mean}	1.78	1.82	1.85	1.87	1.83

2. SAMPLE 1168 (IULIANA QUARRY)

Wavelength (nm)		488	553	590	650	Mean
Acceleration voltage (V)		823	823	823	735	
Reflectance	$R_{\min}$	10.85(10)	9.08(10)	8.88(11)	8.20(11)	9.25
	$R_{\max}$	12.78(9)	11.36(11)	11.89(11)	10.98(9)	11.75
	R_{mean}	11.82	10.22	10.39	9.59	10.50
$\Delta R = R_{\max} - R_{\min}$		1.93	2.28	3.01	2.78	2.50
Bireflectance (Δ R %)		16.33	22.31	28.97	28.99	24.15
Indices of refraction	$n_{\max}$	1.87	1.99	2.01	2.07	1.99
	$n_{\min}$	1.78	1.84	1.82	1.86	1.83
	n_{mean}	1.83	1.92	1.92	1.97	1.91

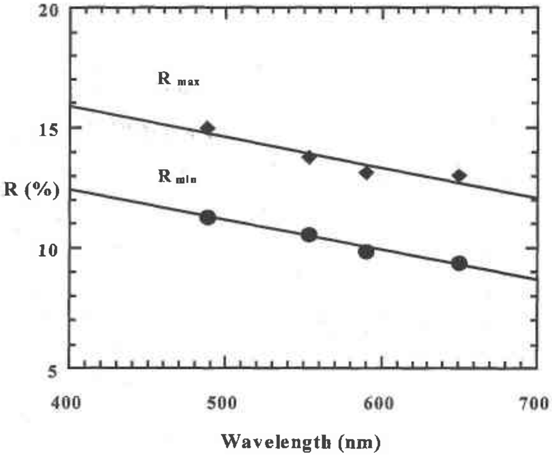

FIG. 3. Reflectance curves drawn for a selected sample of ludwigite from Ocna de Fier (sample 1167).

and n_{max} in the range 1.91–1.99) are lower that the measured values given before, but the maxima compares well with the data of Palache *et al.* (1951).

The density of a representative sample of ludwigite (sample 1168), measured by suspension in Clerici solution diluted with water, is D_m = 3.80(3) g/cm^3. It compares well with the calculated densities in Table 4, derived from chemical compositions and cell volumes, assuming $Z = 4$ (Takéuchi *et al.* 1950). The calculated densities, as well as the measured one, are very similar to the values reported by Aleksandrov (1968) for Al-poor ludwigite with up to 25 mol.% vonsenite in solid solution: $3.74 < D < 3.86$ g/cm^3.

The compatibility indices $1 - (K_P/K_C)$ in Table 4, as derived from Gladstone–Dale calculations, using the specific molar refractivities of oxides given by Mandarino (1976) except for a revised one for B_2O_3 [$k_{B2O3} = 0.241$, as calculated by Mandarino (1981) for boron oxide], may all be classified as excellent or superior (Mandarino 1981). This result is excellent considering the chemical variability of the analyzed samples, for which a constant index of refraction was assumed.

MAGNETIC SUSCEPTIBILITY

Previous studies concerning ludwigite (*i.e.*, Tilley 1951, Leonard *et al.* 1962, Uyeda *et al.* 1963) led to the conclusion that the mineral behaves as a magnetic phase, being probably (weakly) ferromagnetic. This property explains the attraction to the hand magnet reported by Vlisidis & Schaller (1974), but may also be due to contamination by magnetite. A preliminary measurement of the magnetic susceptibility of fine-grained powders prepared by careful hand-picking and heavy-liquid separation indicates, on the basis of the attraction exerted by the Franz isodynamic separator, that the value of susceptibility is always greater than $6000 \bullet 10^6$ e.m.u. This value indicates a magnetic phase, but the magnetic susceptibility (MS) must be anisotropic. The study of MS anisotropy on a cube 2 cm on an edge cut from an apparent monomineralic mass of ludwigite was consequently undertaken. The instrument used was an ac-bridge KLY/2; Hrouda (1982) described the technique that was followed.

AMS measurements are approximated by the second-rank tensor k_{ij}, which may be thought of as a combination of the effects induced by all the magnetic grains within a sample. The three main components of the k_{ij} tensor give the susceptibility values k_1 (maximum), k_2 (medium) and k_3 (minimum). The values recorded for the measured sample (1168) are $k_1 = 12511.76 \bullet 10^6$ e.m.u., $k_2 = 11727.85 \bullet 10^6$ e.m.u. and $k_3 = 9060.39 \bullet 10^6$ e.m.u., the mean susceptibility being $k = 11100 \bullet 10^6$ e.m.u.. The k_{ij} anisotropy obtained on the basis of these values is characterized by the following factors (notations after Uyeda *et al.* 1963): $P = k_1 / k_3 = 1.381$; $L = k_1 / k_2 = 1.067$ et $F = k_2 / k_3 = 1.294$. The ellipsoid that approximates this effect is clearly oblate; Uyeda *et al.* (1963) found a nearly prolate ellipsoid. The maximum value of susceptibility (k_1) was found to be parallel to the fibers, as reported by Uyeda *et al.* (1963). Ludwigite thus is (ferro)magnetic and behaves as a sum of magnetic needles; magnetite grains preferentially disposed along the "separation lines" described earlier induce most probably the weak ferromagnetism as well as the shape effect of anisotropy. This last hypothesis is supported by the fact that magnetite was identified by X-ray diffraction in the powder that resulted from grinding the cube used for measurements.

The data collected here do not allow any conclusion to be drawn about the magnetic behavior of ludwigite itself. A Mössbauer study was undertaken to solve the problem.

MÖSSBAUER SPECTROSCOPY

Mössbauer spectra were recorded for two representative samples of ludwigite from Ocna de Fier. The Mössbauer parameters evaluated from both spectra are listed in Table 6, whereas Figure 4 gives the most complex spectrum. The spectra obtained may be described in terms of two or three Zeeman sextuplets (I, II and III in Fig. 4) and of two quadrupole doublets (IV and V in Fig. 4).

The first two Zeeman sextuplets are clearly attributable to the admixed magnetite. Their internal magnetic fields (IMF), calculated with respect to the IMF (330 kOe) of the outermost Zeeman splitting of metallic iron, are H_I = 480–500 kOe and H_{II} = 440–455 kOe, respectively. They are compatible with the values reported by Bauminger *et al.* (1961) for the IMF of ferric (I) iron in octahedral (B) and ferrous (II) iron in tetrahedral (A) structural sites of a perfectly ordered magnetite.

The third Zeeman sextuplet has an internal magnetic field of 410–420 kOe, which is not compatible with any IMF reported for other possible admixed magnetic phases, such as amorphous iron oxides (445–508 kOe according to Murad & Schwertmann 1980), goethite (380–390 kOe according to Bonnin *et al.* 1982) or maghemite (488–499 kOe according to Shinno &

TABLE 6. MÖSSBAUER HYPERFINE PARAMETERS, RELATIVE IRON DISTRIBUTIONS (I) AND SITES ASSIGNMENT FITTED TO THE LUDWIGITE SPECTRA

No.	Sample	Location of iron	I (%)	Δ (mm/s)(1)	δ (mm/s)(2)	Γ (mm/s)(3)
1	1168	$Fe^{2+}Fe^{3+}{}_2O_4$	17.70	-	-	-
		M1 + M2	13.80	-	-	-
		M3	21.70	2.07	1.00	0.36
		M4	46.80	1.09	0.30	0.37
2	1798	$Fe^{2+}Fe^{3+}{}_2O_4$	8.00	-	-	-
		M1 + M2	0.00	-	-	-
		M3	19.60	2.15	0.91	0.33
		M4	72.40	1.34	0.29	0.38

(1) quadrupole splitting

(2) isomer shift

(3) width of the over-all lines

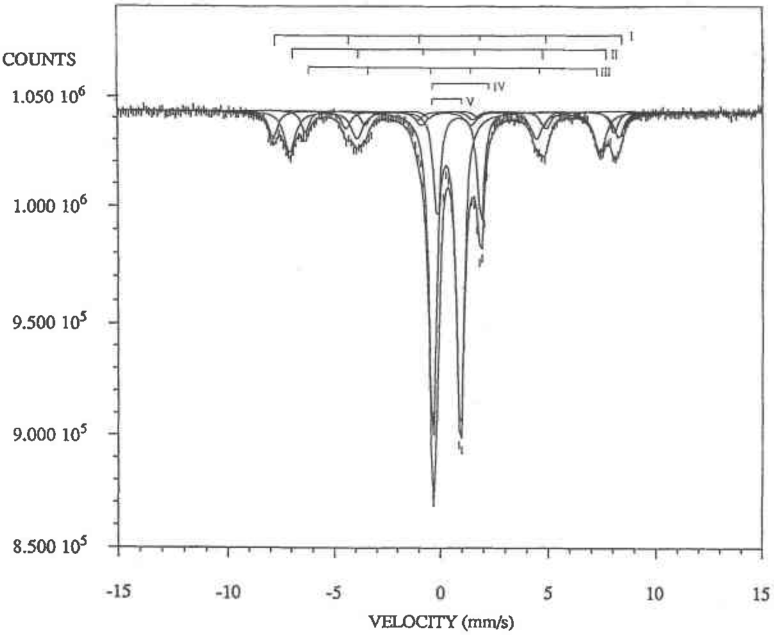

FIG. 4. Room-temperature ^{57}Fe Mössbauer spectrum of a selected sample of ludwigite from Ocna de Fier. Zeeman sextuplets and quadrupole doublets are indicated above the spectra.

Maeda 1989). Kan *et al.* (1984) found such a Zeeman sextuplet in the Mössbauer spectrum of synthetic vonsenite, taken at liquid nitrogen temperature. This third sextuplet thus seems to belong to the ludwigite. Crystal-structure refinements reported by Takéuchi *et al.* (1950), Mokeyeva (1968), Mokeyeva & Aleksandrov (1969) and Irwin & Peterson (1999) show that, in ludwigite, the octahedrally coordinated iron may occupy three different structural sites, namely *M*3 (very regular octahedra), *M*4 (irregular or very distorted octahedra) and *M*1–*M*2 (partially distorted octahedra, in which iron is subordinate to Mg). As supposed by Kan *et al.* (1984), and on the basis of peculiarities of the paramagnetic domain of the spectra, the third Zeeman sextuplet may be assigned to the iron in *M*1–*M*2 sites. This assumption raises the problem of the superparamagnetism of ludwigite. In the Mössbauer spectra reported by Yermakov *et al.* (1969), Malysheva *et al.* (1971), Kurash *et al.* (1972) and Kan *et al.* (1984), as well as in the second spectrum (Table 4), the sextuplet III does not occur. One can expect that the very fine particles of ludwigite obtained after fine grinding and etching with nitric acid (the technique used to obtain the initial powder) will behave superparamagnetically.

The outermost quadrupole doublet in the central (paramagnetic) part of the spectra (IV in Fig. 4) is widely split in comparison with the other doublet (V in Fig. 4). As the quadrupole splitting (Δ) is sensitive to the distribution of cations in the surrounding sites, and as the presence of distorted octahedral sites imply values of $\Delta < 2$ mm/s (Hawthorne 1988), the recorded Δ value, 2.07–2.15 mm/s, is consistent with the iron being located in the most regular octahedron in the structure, namely *M*3. The isomer shift δ recorded for this doublet (0.91–1.00 mm/s) is characteristic of ferrous iron.

The innermost doublet has a lower quadrupole splitting Δ (1.09–1.34 mm/s) and isomer shift δ (0.29–0.30 mm/s), which appear to be consistent with octahedrally coordinated ferric iron in the major distorted octahedral site, *M*4. The low values of δ as compared with those reported by Kurash *et al.* (1972) and Swinnea & Steinfink (1983) for vonsenite, in which Fe^{3+} occupy the attenuated eccentric octahedra, are indicative of ludwigite.

The values of the hyperfine parameters, as well as the sites assignment for the central part of the spectra, are closely similar to those found for natural and synthetic ludwigite by Yermakov *et al.* (1969), Malysheva *et al.* (1971), Kurash *et al.* (1972) and Kan *et al.* (1984).

CHEMICAL DATA

Critical review of previous data

All the existing chemical data on ludwigite from the type locality (Tschermak 1874, Schaller 1911, Codarcea

TABLE 7. RECALCULATION OF PREVIOUSLY REPORTED CHEMICAL DATA ON LUDWIGITE FROM OCNA DE FIER

Sample*	1	2	3	4	5	6	7	8	9
B_2O_3	16.09	15.06	17.02⁽¹⁾	17.50⁽¹⁾	16.13	16.82	16.83	17.46	15.64
Fe_2O_3	39.92	39.29	35.67	33.06	41.85	39.27	36.59	38.20	36.67
FeO	12.46	17.67	15.84	16.39	12.68	10.76	11.02	10.48	18.45
MgO	31.69	26.91	28.88	28.55	29.68	34.76	35.17	33.83	29.18
CO_2	-	-	0.90	-	-	-	-	-	-
SiO_2	-	-	0.36	-	0.36	0.33	0.39	-	-
H_2O^+	-	-	0.82	1.50	-	-	-	-	0.01
H_2O^-	-	-	0.51	3.00	-	-	-	-	-
Total	100.16	98.93	100.00	100.00	100.70	101.94	100.00	99.97	99.95
PROPOSED NORMATIVE COMPOSITIONS (WT.%)									
ludwigite	100.16	98.93	90.17	83.41	99.86	101.17	99.09	99.97	99.85
serpentine	-	-	0.83	-	-	-	-	-	-
siderite	-	-	2.37	-	-	-	-	-	-
szaibelyite	-	-	6.63	13.59	-	-	-	-	0.10
forsterite	-	-	-	-	0.84	0.77	0.91	-	-
H_2O	-	-	0.51	3.00	-	-	-	-	-
DEDUCED COMPOSITIONS OF LUDWIGITE (WT.% OXIDES)⁽²⁾									
B_2O_3	16.064	15.223	15.528	13.607	16.153	16.625	16.985	17.465	15.622
Fe_2O_3	39.857	39.715	39.951	41.938	41.908	38.816	36.926	38.211	36.721
FeO	12.440	17.861	16.094	19.062	12.698	10.636	11.121	10.483	18.476
MgO	31.639	27.201	28.427	25.393	29.241	33.923	34.968	33.841	29.181
CATIONS ON THE BASIS OF 5 (O)									
B	0.962	0.940	0.950	0.861	0.973	0.981	0.997	1.021	0.957
Fe^{3+}	1.040	1.069	1.065	1.157	1.100	0.998	0.945	0.974	0.981
Fe^{2+}	0.361	0.534	0.477	0.585	0.370	0.304	0.316	0.297	0.548
Mg	1.636	1.451	1.501	1.388	1.521	1.728	1.772	1.709	1.544
VONSENITE CONTENT IN THE SOLID SOLUTION (MOL.%)									
reported⁽³⁾	17.75	27.00	24.45	19.32	24.36	14.67	14.95	14.77	32.50
corrected	18.07	26.90	24.12	29.65	19.57	14.96	15.13	14.81	26.20

* Analyses given as follows: 1 and 2 by Tschermak (1874), 3 by Schaller (1911), 4 by Koch (1960), 5-9 by Codarcea *et al.* (1957) and Kissling (1967).

(1) - deduced by difference;

(2) - totals recalculated to 100%;

(3) - excepting 4 (calculated without subtraction of impurities), values given by Kissling (1967).

et al. 1957, Koch 1960, Kissling 1967) were obtained by wet-chemical analysis. These results indicate a low content of vonsenite in solid solution (up to 30 mol.%). None of the data, not even those which permitted Tschermak (1874) to deduce the correct formula, are stoichiometric, *i.e.*, with a *Me*O:Me$_2$O$_3$:B$_2$O$_3$ molar ratio of 4:1:1. Some of the previously reported compositions (Table 7) contain small quantities of SiO_2, H_2O^+, and CO_2, which are consistent with the presence of admixed minerals (*e.g.*, szaibelyite, serpentines, forsterite, carbonates, and hydrated oxides of iron). As can be seen in Table 7, none of the existing compositions take into consideration the presence of Al, Ti and Sn, for example. Ludwigite is, however, a chemically complex mineral, with a large number of possible substitutions; a structural formula may be represented by $(M1\text{–}3)_2M4(BO_3)O_2$, with $M1$–3 representing Mg and Fe^{2+} but also Ni and Mn^{2+}, and $M4$ representing Fe^{3+}, Al, Ti^{4+}, Sn^{4+}, Cr^{3+}, Mn^{3+}, Sb^{5+} but also Mg or Fe^{2+} (where coupled with cations with higher charge). Ludwigite may contain large quantities of Al; aluminian ludwigite, with 10.97–12.70 wt.% Al_2O_3, was described by Schaller & Vlisidis (1961), Pertsev & Aleksandrov (1964), Kanishchev & Pertsev (1969). It may also contain Ti; Konev *et al.* (1970) described a sample of titanian ludwigite containing 7.35 wt.% TiO_2.

Subtracting stoichiometric minerals in order to eliminate SiO_2 (in forsterite and serpentines), H_2O (in serpentines and szaibelyite), CO_2 (in siderite), it is possible to derive chemical compositions corresponding to "pure" ludwigite. It is of note, however, that in spite of the lack of determinations for Al, Sn, Ti, Sb, Mn, many of the ludwigite samples in Table 7 are Fe^{3+}-oversaturated; Fe^{3+} exceeds 1 atom per formula unit (*apfu*), regardless of whether the formula is calculated with respect to cations or a fixed number of oxygen atoms

TABLE 8. RESULTS OF WET-CHEMICAL ANALYSES OF SELECTED SAMPLES OF LUDWIGITE FROM OCNA DE FIER*

Sample	1167	1168	1417	1418	1439	1798	1982	2037
SiO_2	0.35	0.43	0.49	0.46	0.60	0.62	0.94	0.38
TiO_2	0.67	0.12	0.05	0.06	0.07	0.22	0.12	0.21
B_2O_3	17.21	17.74	17.43	17.88	17.74	17.60	17.48	17.20
Al_2O_3	0.22	0.50	0.62	0.31	0.61	0.45	0.49	0.42
Fe_2O_3	38.21	38.18	39.00	37.80	37.90	36.93	37.33	38.77
FeO	3.23	4.73	3.17	4.18	7.14	4.88	5.21	5.01
MgO	38.55	37.76	39.12	38.22	35.89	38.04	37.22	36.95
MnO	0.34	0.25	0.33	0.12	0.12	0.22	0.11	0.12
CaO	0.09	0.14	0.11	0.08	0.14	0.15	0.06	0.36
H_2O^+	0.11	0.21	0.15	0.27	0.21	0.32	0.50	0.24
H_2O^-	0.07	-	-	0.33	-	0.18	0.08	0.21
TOTAL	99.05	100.06	100.47	99.71	100.42	99.61	99.54	99.87
PROPOSED NORMATIVE COMPOSITIONS (WT.%)								
ludwigite	98.17	98.28	99.34	97.01	98.21	96.79	95.33	95.33
magnetite	-	-	-	-	-	-	-	2.33
serpentine	0.81	0.99	1.13	1.06	1.38	1.43	2.17	0.88
szaibelyite	-	0.79	-	1.31	0.83	1.21	1.96	1.12
H_2O	0.07	-	-	0.33	-	0.18	0.08	0.21
DEDUCED COMPOSITIONS OF LUDWIGITE (WT.% OXIDES)**								
B_2O_3	17.53	17.72	17.56	17.87	17.66	17.67	17.49	17.56
TiO_2	0.68	0.12	0.05	0.06	0.07	0.23	0.13	0.22
Al_2O_3	0.22	0.51	0.62	0.32	0.62	0.47	0.51	0.44
Fe_2O_3	38.92	38.85	39.26	38.96	38.59	38.15	39.16	38.98
FeO	3.29	4.81	3.19	4.31	7.27	5.04	5.47	4.50
MgO	38.92	37.60	38.88	38.28	35.53	38.06	37.06	37.79
MnO	0.35	0.25	0.33	0.12	0.12	0.23	0.12	0.13
CaO	0.09	0.14	0.11	0.08	0.14	0.15	0.06	0.38
CATIONS ON THE BASIS OF 5 (O)								
B	0.996	1.011	0.997	1.016	1.018	1.008	1.003	1.002
Ti	0.017	0.003	0.001	0.001	0.002	0.006	0.003	0.005
Al	0.009	0.020	0.024	0.012	0.024	0.018	0.020	0.017
Fe^{3+}	0.964	0.966	0.972	0.966	0.969	0.949	0.979	0.970
Fe^{2+}	0.091	0.133	0.088	0.119	0.203	0.139	0.152	0.124
Mg	1.910	1.853	1.907	1.880	1.768	1.875	1.835	1.863
Mn	0.010	0.007	0.009	0.003	0.003	0.006	0.003	0.004
Ca	0.003	0.005	0.004	0.003	0.005	0.005	0.002	0.013
ISOMORPHISM IN M1-M3 SITES								
ludwigite	95.45	93.30	95.59	94.05	89.70	93.10	92.35	93.76
vonsenite	4.55	6.70	4.41	5.95	10.30	6.90	7.65	6.24
ISOMORPHISM IN M4 SITES								
ludwigite	97.37	97.68	97.49	98.67	97.39	97.53	97.70	97.78
Mg_2AlBO_5	0.91	2.02	2.41	1.23	2.41	1.85	2.00	1.71
azoproite	1.72	0.30	0.10	0.10	0.20	0.62	0.30	0.51

* results expressed in wt.%

** totals recalculated to 100%

(5 O in Table 7). The presence of admixed magnetite or hematite–maghemite can explain this finding. For the samples that are Fe^{3+}-depleted, the molar ratio $Me^{2+}O/B_2O_3$ is very high, which also indicates the presence of oxide impurities. The previous analyses were thus made on impure material, which supports the idea that the proportions of the vonsenite component reported so far for the ludwigite from Ocna de Fier are inexact. New analyses were thus deemed necessary for a better characterization of the mineral.

Results of new wet-chemical analyses

The primary results of new wet-chemical analyses are given in Table 8. They show the persistence of small quantities of SiO_2, H_2O and, in some cases, a higher concentration of Fe than necessary for the stoichiometry, owing to the presence of impurities such as forsterite, serpentines, szaibelyite and magnetite. Subtraction of constituents to compensate for these minerals in order to eliminate SiO_2 and H_2O is easy, but the presence of iron in excess imposes that all other elements are relatively depleted upon recalculation of the formula. It is, however, possible to quantify a correction, admitting that stoichiometric magnetite may be subtracted in a straightforward manner, to obtain more accurate MeO:Me_2O_3:B_2O_3 proportions. A proposed normative composition is then given for all samples in Table 8.

The derived compositions in Table 8 represent in fact mean compositions at the scale of a sample. As the chemical composition of ludwigite within individual samples is rather uniform (see below), the compositions in Table 8 are considered to fit well with the compositions of the individual grains. The corresponding chemical-structural formulae were calculated on the basis of five atoms of oxygen. The formulae indicate that: (1) ludwigite from Ocna de Fier is closer to the magnesian end-member than previously reported. It contains molar percentages of vonsenite ranging from 4.41 to 10.30%. (2) The very low contents of Mn (up to 0.010 *apfu*) and Ca (up to 0.013 *apfu*) compare well with similar data in literature (Aleksandrov 1961, 1982, Leonard *et al.* 1962, Vlisidis & Schaller 1974). (3) The compositional variation in the *M*4 structural position appears to be insignificant. The occupancy of these sites by Fe^{3+} is between 97.37 and 98.67%, with low contents of Ti (*cf.* azoproite) and Al (*cf.* Mg_2AlBO_5), up to 1.72 and 2.41 mol.%, respectively.

The numerous possible substitutions within the ludwigite group necessitated chemical investigations of the concentrations in Sn, Sb, Cr, Ni, Co, and Zn. The concentration of Sb (*cf.* chestermanite) and Sn was determined by inductively coupled plasma – mass spectrometry, and that of Ni (*cf.* bonaccordite), Co, Zn and Cr, by inductively coupled plasma – atomic emission spectrometry. Between 3.7 and 12.0 ppm Sn, 68.6 and 123.4 ppm Sb, 8.7 and 13.3 ppm Ni, 23.9 and 65.1 ppm Co, 190.1 and 880.1 ppm Zn, and 11.4 and 60.1 ppm Cr were detected in various samples, which appears to not exert a significant influence on the mineral chemistry. It is of note, however, that the most distinctive feature of the Ocna de Fier ludwigite is the higher content in Sb and the lower content in Sn than in other examples of ludwigite in Romania (Marincea 1998).

Electron-microprobe analyses

Electron-microprobe analyses of selected samples of ludwigite from Ocna de Fier were made in order to complete the chemical data. Representative results are summarized in Table 9. The variation in composition of individual crystals in the same specimen being negligible, compositions in Table 9 are given as average results of random spot analyses. It is of note that the back-scatter electron detector does not indicate any chemical zoning of the analyzed grains. The amount of Fe_2O_3 has been calculated with the assumption that the

TABLE 9. RESULTS OF ELECTRON-MICROPROBE ANALYSES OF SELECTED SAMPLES OF LUDWIGITE FROM OCNA DE FIER(1)

Sample	1168	1415	1439	1799	1866	1867	1891	1975	2073	2218	2219	2221
No.(2)	9	7	11	10	15	10	6	10	3	10	7	11
B_2O_3	16.900	17.813	17.749	17.425	17.923	17.672	17.775	17.771	17.723	17.192	17.496	17.690
TiO_2	0.034	0.017	0.014	0.026	0.017	0.040	0.042	0.011	0.040	0.092	0.038	0.049
Al_2O_3	0.663	0.343	0.308	0.424	0.349	1.652	1.600	1.417	0.457	0.412	0.467	0.699
Fe_2O_3(3)	38.817	37.590	37.656	39.685	37.803	36.645	36.468	36.984	37.437	39.958	38.222	37.098
FeO(3)	9.925	6.619	7.102	4.564	4.938	6.715	6.381	5.767	7.319	5.562	7.253	7.803
MgO	33.430	37.421	37.038	37.671	38.703	37.000	37.368	37.735	36.809	36.565	36.302	36.491
MnO	0.185	0.163	0.105	0.184	0.242	0.276	0.314	0.294	0.181	0.197	0.102	0.170
CaO	0.046	0.034	0.028	0.021	0.025	0.000	0.052	0.021	0.034	0.022	0.120	0.000
Total	100.00	100.00	100.00	100.00	100.00	100.00	100.00	100.00	100.00	100.00	100.00	100.00
CATIONS ON THE BASIS OF 5 (O)												
B	0.991	1.020	1.019	0.997	1.019	1.009	1.013	1.012	1.018	0.990	1.009	1.017
Ti	0.001	0.000	0.000	0.001	0.000	0.001	0.001	0.000	0.001	0.002	0.001	0.001
Al	0.027	0.013	0.012	0.017	0.014	0.064	0.062	0.055	0.018	0.016	0.018	0.027
Fe^{3+}	0.993	0.939	0.943	0.990	0.937	0.912	0.906	0.918	0.938	1.003	0.961	0.930
Fe^{2+}	0.282	0.184	0.198	0.127	0.136	0.186	0.176	0.159	0.204	0.155	0.203	0.217
Mg	1.694	1.851	1.837	1.861	1.901	1.825	1.839	1.855	1.827	1.819	1.807	1.813
Mn	0.005	0.005	0.003	0.005	0.007	0.008	0.009	0.008	0.005	0.006	0.003	0.005
Ca	0.002	0.001	0.001	0.001	0.001	0.000	0.002	0.001	0.001	0.001	0.004	0.000
ISOMORPHISM IN M1-M3 SITES												
ludwigite	85.73	90.96	90.27	93.61	93.32	90.75	91.27	92.11	89.96	92.15	89.90	89.31
vonsenite	14.27	9.04	9.73	6.39	6.68	9.25	8.73	7.89	10.04	7.85	10.10	10.69
ISOMORPHISM IN M4 SITES												
ludwigite	97.26	98.63	98.74	98.21	98.53	93.35	93.50	94.35	98.01	98.24	98.06	97.08
Mg_2AlBO_5	2.64	1.37	1.26	1.69	1.47	6.55	6.40	5.65	1.89	1.57	1.84	2.82
azoproite	0.10	0.00	0.00	0.10	0.00	0.10	0.10	0.00	0.10	0.20	0.10	0.10

(1) Results expressed in wt.%. Samples from Magnet (1415, 1439, 1799, 2218, 2219, 2221), Arhangheli (1867, 1891, 1975, 2073) and Iuliana (1168, 1866) quarries.

(2) number of point analyses.

(3) as calculated.

molar ratio B_2O_3/(FeO + MgO + MnO + CaO) is equal to 1/4, after assigning all Mg, Ca and Mn to fill the sites *M*1–*M*3. Using this method, most of the analyzed samples of ludwigite are found to be Fe^{3+}-depleted, which is consistent with the presence of Al, Ti^{4+}, Sb^{5+}, Sn^{4+}, Cr^{3+} at the *M*4 sites.

In all cases, the ludwigite is very magnesian, ranging in composition from 85.7 to 93.6% of the end member. The ludwigite at Ocna de Fier thus shows only a limited proportion of the vonsenite component. As shown by the wet-chemical data, it contains low levels of the azoproite and Mg_2AlBO_5 components: up to 0.20 mol.% and up to 6.55 mol.%, respectively.

X-RAY POWDER-DIFFRACTION DATA

X-ray powder-diffraction patterns were obtained for several samples of ludwigite from Ocna de Fier. The main observed (*hkl*) reflections, as well as the cell parameters refined using the least-squares computer program of Appleman & Evans (1973), as revised for microcomputer use by Benoit (1987), are listed in Table 10. Marincea (1998) provided the complete set of X-ray data.

As observed by Aleksandrov (1968, 1982) for natural samples of ludwigite and by Xie *et al.* (1985) for synthetic material, the position of the lines of a ludwigite X-ray pattern is strongly dependent on the ratio $Fe^{2+}/(Fe^{2+}+Mg)$ of the analyzed samples. It is evident that the advance of the substitution of Fe^{2+} for Mg causes a significant shift toward higher values of *d*. As can be seen in Table 10, a direct correlation between the *d* values and $X_{Fe} = Fe^{2+}/(Fe^{2+}+Mg)$ may be observed, but is very poor for the analyzed samples of ludwigite. Another factor, namely Al-for-Fe^{3+} substitution, exerts an opposite influence on the position of the reflections. Bonazzi & Menchetti (1989), discussed the importance of the factor $X_{Al} = Al/(Al+Fe^{3+})$ on the cell parameters.

Note that the unit-cell parameters in Table 10 are in close agreement with those already in the literature for magnesian ludwigite with low contents of Al. The values previously reported by Bonazzi & Menchetti (1989) for ludwigite from Ocna de Fier [*e.g.*, *a* 9.252(2), *b* 12.315(2), *c* 3.038(1) Å for samples VA and MO] are also in very good agreement with the values in Table 10. Authors of previous studies (*i.e.*, Aleksandrov 1968, 1982, Xie *et al.* 1985, Bonazzi & Menchetti 1989) showed that chemical parameters, and particularly X_{Fe},

TABLE 10. DIFFRACTOMETRIC *VERSUS* CHEMICAL PARAMETERS OF OCNA DE FIER LUDWIGITE(1)

Sample	*d*(201)	*d*(211)	*d*(241)	*d*(331)	*d*(341)	*d*(441)	*d*(561)	*d*(712)	*a* (Å)	*b* (Å)	*c* (Å)	*V* (Å^3)	X_{Fe}	X_{Al}	*k*
1167*	2.5347	2.4951	1.9524	-	1.7691	1.5783	1.2498	0.9980	9.233(8)	12.243(9)	3.057(3)	345.537	0.046	0.009	9.639
1168*	2.5470	2.4959	1.9582	1.9143	1.7730	1.5793	1.2515	0.9980	9.263(6)	12.317(5)	3.042(3)	347.078	0.067	0.020	9.550
1415$^{\blacklozenge}$	2.5493	2.4961	1.9584	1.9178	1.7655	1.5816	1.2522	0.9976	9.290(6)	12.234(8)	3.050(2)	346.670	0.090	0.014	9.254
1417*	2.5354	-	1.9564	1.9131	1.7749	1.5791	1.2517	0.9982	9.260(4)	12.334(6)	3.033(4)	346.448	0.044	0.024	9.824
1418*	2.5368	-	1.9570	1.9134	1.7735	1.5792	1.2515	-	9.250(7)	12.321(5)	3.034(5)	345.780	0.060	0.012	9.532
1439*	2.5376	-	1.9583	1.9142	1.7732	1.5796	-	0.9978	9.260(4)	12.326(5)	3.037(2)	346.664	0.103	0.024	9.234
1798*	2.5470	2.5342	1.9558	1.9117	1.7714	1.5780	1.2514	0.9973	9.256(7)	12.233(9)	3.057(3)	346.188	0.069	0.019	9.519
1799$^{\blacklozenge}$	2.5524	2.5099	-	1.9168	-	1.5773	1.2513	0.9976	9.236(7)	12.301(8)	3.053(3)	346.927	0.064	0.008	9.448
1866$^{\blacklozenge}$	2.5436	2.4946	-	1.9146	-	1.5807	1.2517	0.9994	9.276(9)	12.242(8)	3.049(3)	346.281	0.067	0.015	9.495
1867$^{\blacklozenge}$	2.5486	2.4950	1.9592	1.9166	1.7657	1.5801	-	0.9970	9.258(9)	12.255(8)	3.053(3)	346.345	0.093	0.066	9.796
1872$^{\blacklozenge}$	2.5597	2.4951	1.9535	1.9095	-	1.5767	1.2505	0.9978	9.225(8)	12.267(9)	3.057(3)	345.991	-	-	-
2218$^{\blacklozenge}$	2.5540	2.4960	1.9600	1.9167	1.7711	1.5754	1.2510	0.9975	9.247(6)	12.259(8)	3.056(2)	346.435	0.079	0.016	9.386

(1) Chemical computations were carried out on the basis of wet-chemical (*) or electron-microprobe ($^{\blacklozenge}$) analyses. The (observed) *d* spacings are given in Å.

exert an important influence on the cell dimensions. The parameters *a* and *V* depend especially strongly on the extent of Mg-for-Fe^{2+} substitution (Aleksandrov 1968, 1982), and increase with X_{Fe}, but they are also sensitive to the extent of Al-for- Fe^{3+} substitution (Marincea 1998). A discussion of the behavior of the cell volume as a function of chemical variability may be useful in understanding the dispersion of values in Table 10.

Taking into account the differences in ionic radii among ^{VI}Mg, ^{VI}Fe^{2+}, ^{VI}Fe^{3+} and ^{VI}Al, it is evident that the substitution of Fe^{2+} for Mg will increase the cell volume, whereas the substitution of Al for Fe^{3+} will decrease it. One may use the comprehensive factor *k* as an expression of the difference in the steric hindrance between the cations entering the octahedral sites in the structure, as proposed by Bonazzi & Menchetti (1989). The value of *k* may be calculated as:

$$k = \{2[r(^{VI}Fe^{2+}) - r(^{VI}Mg)]\bullet(1 - X_{Fe}) + [r(^{VI}Fe^{3+}) - r(^{VI}Al)]\bullet X_{Al}\}\bullet 100\ (\%).$$

Using the ionic radii given by Shannon & Prewitt (1969) for the four cations [$r(^{VI}Fe^{2+}) = 0.770$ Å, $r(^{VI}Mg) = 0.720$ Å, $r(^{VI}Fe^{3+}) = 0.645$ Å and $r(^{VI}Al) = 0.535$ Å], the *k* value may be calculated as: $k\ (\%) = 10 + 11\ X_{Al} - 10\ X_{Fe}$.

The values obtained for samples from Ocna de Fier are given in Table 10. As shown in Figure 5, and in perfect agreement with the data of Bonazzi & Menchetti (1989), a poor inverse correlation between *k* and *V* is established, which best explains the variability of the *V* values. A similar correlation may be established between *k* and *c*, whereas a less regular behavior is observed for *a* and *b* parameters.

THERMAL BEHAVIOR

Data concerning the thermal behavior of ludwigite are scarce because the mineral is expected to have a high melting point (up to 1000°C), and no structural changes can be expected below this temperature. Note that a thermal analysis of "ludwigite" was reported by Hang (1957) and is mentioned by Smothers & Chiang (1966), but it was obviously made on impure (mainly szaibelyite-bearing) material, as proven by the chemical data provided. The admixed szaibelyite is clearly responsible at least for the strong endothermic effect at 725°C observed by Hang (1957).

Taking into account the data reported above, it is surprising that Kissling (1967), on the basis of a DTA curve for a sample of ludwigite from Ocna de Fier, stated that the mineral breaks down to kotoite, magnetite and hematite at a temperature below 1000°C. Complete sets of thermal curves were consequently recorded for many samples of ludwigite from the type locality, using the same operating conditions as Kissling (1967). DTA and DTG curves are reproduced in Figure 6.

The sole effect attributable to the ludwigite itself is the flat exothermic peak centered at about 650°C. Because endothermic effects are not to be expected, the main effects of this type were assigned to different admixed minerals by analogy with data on pure materials

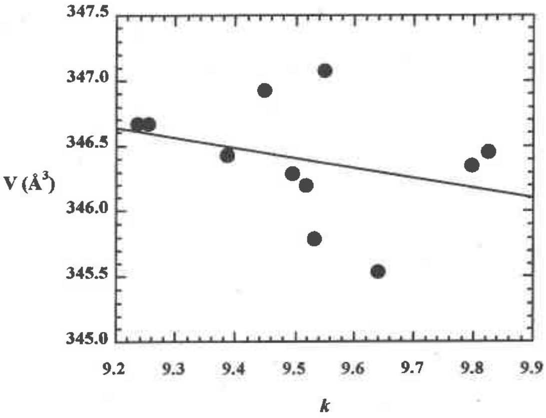

FIG. 5. Correlation between cell volume and *k* chemical factor, as established for ludwigite from Ocna de Fier.

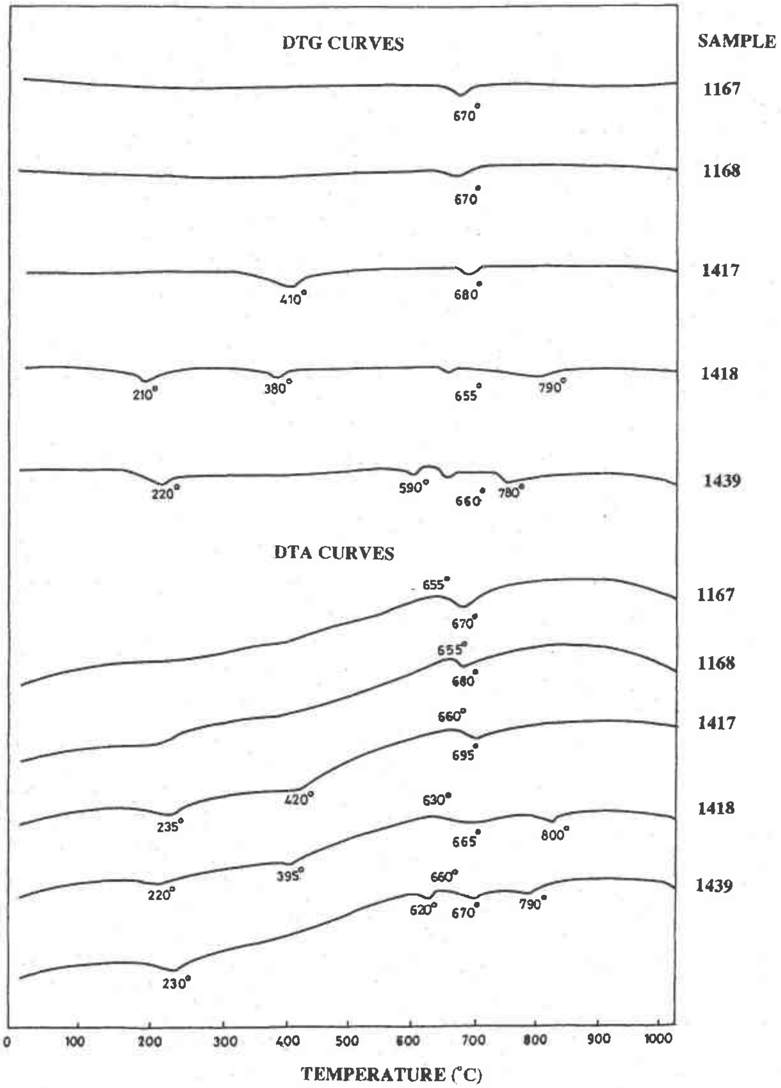

FIG. 6. Thermal curves recorded for selected samples of ludwigite from Ocna de Fier: differential thermogravimetric (top) and differential thermal analysis (bottom).

reported for hydrated ferric oxides of gel type (Gheith 1952, Ammou-Chokroum & Pianelli 1970), goethite (Kauffman & Dilling 1950, Ammou-Chokroum & Pianelli 1970), antigorite (Caillère 1936), szaibelyite (Watanabe 1953, Shabynin 1955) and calcite (Kauffman & Dilling 1950), taking into account the slight shifts in temperature due to the admixture (Todor 1972). The assignment of the main thermal effects, together with the losses in weight recorded on the TGA curves, are given in Table 11. The presence of the admixed phases given in the table, supported by optical and diffractometric data, raises the problem of the correct assumption of the broad exothermic effect mentioned before. The most probable structural cause of this exothermic effect is the oxidation of the ferrous to ferric iron, but it is not possible to specify if this iron pertains to ludwigite or to admixed magnetite. Kissling (1967) mentioned a similar effect, but it was not assigned to any structural change. In magnetite, the analogous effect occurs between 625 and 675°C, and corresponds, according to Gheith (1952) and Schmidt & Vermaas (1955), to the change of γ-Fe_2O_3 (maghemite) to α-Fe_2O_3 (hematite). A first exothermic effect, marking the superficial oxidation of magnetite, which produces maghemite over

TABLE 11. THERMAL DATA FOR ADMIXED MINERALS IN HAND-PICKED LUDWIGITE

Sample	Type of effect	Temperature of the effect (°C) on DTA	on DTG	Loss in weight on the TGA curve (wt.%)	Revealed mineral
1167	exothermic	655	-	-	magnetite
	endothermic	670	660	1.75*	szaibelyite
1168	exothermic	655	-	-	magnetite
	endothermic	680	670	1.55*	szaibelyite
1417	endothermic	235	220	1.20	hydrated ferric oxide
	endothermic	420	410	2.35	goethite
	exothermic	660	-	-	magnetite
	endothermic	695	680	0.30*	szaibelyite
1418	endothermic	220	210	0.50	hydrated ferric oxide
	endothermic	395	380	1.55	goethite
	exothermic	630	-	-	magnetite
	endothermic	665	655	0.35*	szaibelyite
	endothermic	800	790	1.20	calcite
1439	endothermic	230	220	1.25	hydrated ferric oxide
	endothermic	620	590	2.25*	antigorite
	exothermic	660	-	-	magnetite
	endothermic	670	660	1.20*	szaibelyite
	endothermic	790	780	0.30	calcite
Kissling (1967)	endothermic	230	-	-	hydrated ferric oxide
	exothermic	678	-	-	magnetite

* reduced by the increase in weight due to the magnetite oxidation.

the interval 280–375°C, according to Gheith (1952) and Schmidt & Vermaas (1955), may be inhibited in samples with large particle sizes, such as those used in this study (Egger 1963). On the other hand, taking into account the thermal behavior of vonsenite, which breaks down to hematite and amorphous $Fe_2B_2O_5$ at 764°C (Galan *et al.* 1981), one can expect that below this temperature, ludwigite remains unchanged. It thus seems that the exothermic effect centered at about 650°C can be assigned to the oxidation of magnetite.

A supplementary investigation of the thermal behavior of ludwigite was undertaken by recording the XRD pattern as heating in air progressed up to 1000°C. The main reflections of this mineral may be clearly recognized in the powder patterns recorded at 200, 400, 600 and 800°C. A broadening of peaks occurs at 1000°C, proving an incipient fusion and the amorphization of the mineral. Marincea (1998) listed the complete set of diffraction lines. The assertion of Kissling (1967) concerning the breakdown into kotoite, magnetite and hematite should be considered with caution.

INFRARED ANALYSIS

Infrared absorption spectra of selected samples of ludwigite from Ocna de Fier were recorded between 250 and 4000 cm^{-1}, before and after heating at 1000°C. In the spectra given in Figure 7, the high-wavenumber domain between 1700 and 4000 cm^{-1} is not reproduced because of the anhydrous character of ludwigite. A complete list of absorption bands recorded for many samples is given in Table 12.

As expected, the most significant absorption bands in the mid-wavenumber region (600 to 1350 cm^{-1}) may be assigned to vibrations belonging to the (BO_3) group. These absorption bands (cm^{-1}) are assigned as follows: 1300–1335 and 1260–1268: asymmetric stretching; 920–940: symmetric stretching; 704–708: out-of-plane bending; 622–630: in-plane bending. The latter should in principle be doubly degenerate, but the band at 560–570 cm^{-1} could not be unequivocally assigned because the theoretical superposition of the Fe^{3+}–O stretching. The band assignments given above are coincident with those reported for ludwigite by Aleksandrov *et al.* (1965), Nekrasov & Brovkin (1966) and Xie *et al.* (1985). An analysis of the factor-group splitting show that the splitting of both asymmetric stretching and in-plane bending is consistent with a $C_{3\nu}$ or C_s point symmetry of BO_3 (Duval & Lecompte 1952, Steele & Decius 1956), which implies that this molecular group

TABLE 12. POSITIONS AND ASSIGNMENTS OF THE INFRARED BANDS RECORDED FOR SELECTED SAMPLES OF LUDWIGITE FROM OCNA DE FIER*

Moenke (1962)(1)	Sample 1167	1168	1417	1418	1439	1798	1866	1982	2037	2218	Assignment
1630	1630	1618	1630	1616	1635	1612	1620	1610	1630	1630	δ H_2O
-	1460	1440	1390	1432	1420	1436	1420	1420	1420	1430	δ H_2O
1300	1320	1305	1305	1300	1310	1300	1300	1300	1340	1335	ν_3 BO_3
1265	1264	1264	1268	1268	1266	1268	1260	1268	1268	1262	ν_3' BO_3
-	940	938	935	935	935	935	920	935	920	920	ν_1 BO_3
-	795	794	795	795	800	798	795	790	794	798	B-O-^{VI}Me (?)
701	706	704	704	704	704	708	704	706	704	704	ν_2 BO_3
625	626	620	626	625	630	628	630	622	630	622	ν_4 BO_3
-	-	-	610	-	620	620	620	615	-	-	B-O-^{VI}Me (?)
520	565	564	570	565	570	560	560	560	566	570	ν_4' BO_3 (?)
-	538	530	520	535	525	-	535	540	-	-	
	510	-	-	-	510	520	522	525			
480	484	480	490	485	490	480	476	486	480	495	
440	438	430	432	440	442	435	440	436	432	432	Mainly
415	402	392	408	410	410	410	404	402	410	415	^{VI}Me - O
-(2)	342	330	340	330	330	330	330	320	330	330	
-	320	318	318	318	320	318	320	-	312	318	
-	300	295	295	295	300	290	295	298	305	305	
-	272	273	260	275	270	275	272	274	280	278	

* wavenumbers in cm^{-1}

(1) as given for a sample of ludwigite from Ocna de Fier, of unknown composition.

(2) not recorded below 400 cm^{-1}.

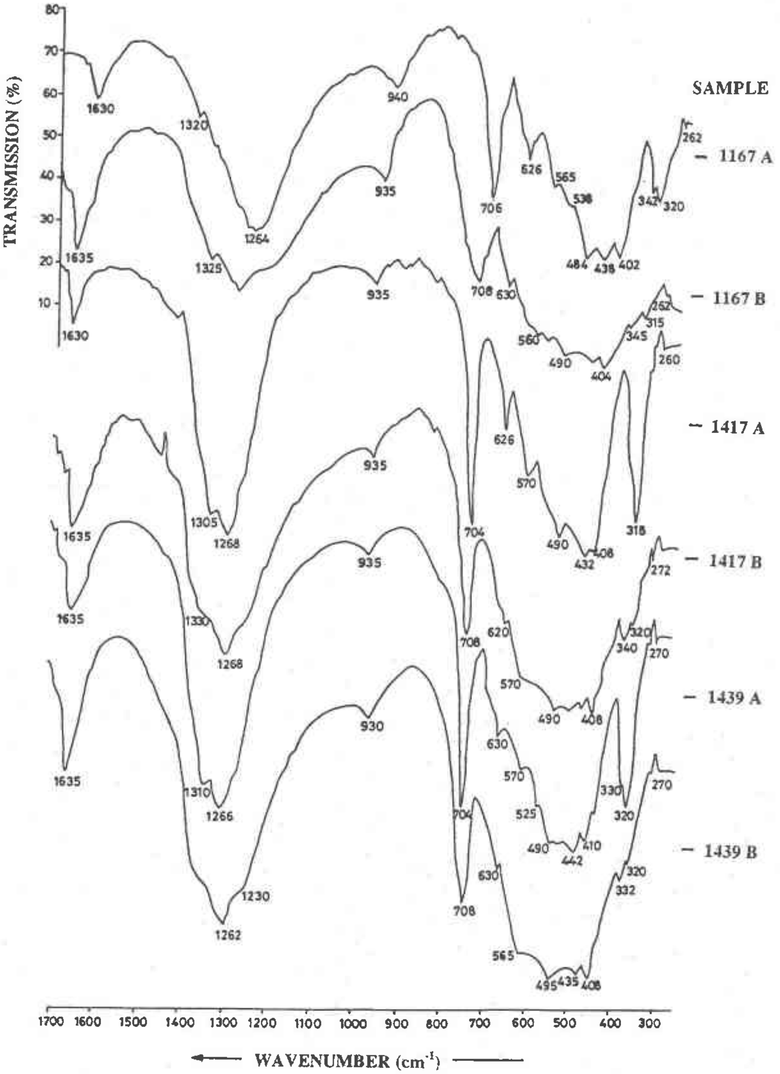

FIG. 7. Infrared spectra of selected samples of ludwigite from Ocna de Fier before (A) and after (B) heating at 1000°C, in air.

is non-planar. As this kind of behavior is characteristic for (magnesian) ludwigite, in opposition with vonsenite, in which BO_3 has a clear D_{3h} (planar) symmetry (Aleksandrov *et al.* 1965, Nekrasov & Brovkin 1966, Xie *et al.* 1985), the infrared analysis confirms the low contents in ferrous iron reported earlier. Note that the effect of composition does not appear to be evident in details of band positions and intensities in the recorded spectra.

The spectra of heated ludwigite (Fig. 7) are similar in all respects with those of unheated samples, which indicates the same basic structure. Minor differences do occur, however, in the low-wavenumber region (250 to 600 cm^{-1}), and consist in the broadening of the background of the continuum of bands in this region. The partial oxidation of the admixed magnetite must displace the Fe^{3+}–O vibrations toward lower wavenumbers, as at the transition magnetite – hematite. As observed by Liese (1967), the main absorption band (probably the Fe^{3+}–O stretching) is centered near 570 cm^{-1} in pure magnetite, and around 530 cm^{-1} in pure hematite, whereas in mixtures of magnetite and hematite, the corresponding band may be found between 530 and 570 cm^{-1}. After heating, the absorption bands corresponding to stretching and bending modes of Fe^{3+}–O bonds in magnetite should be reduced in intensity, vanish or decrease in wavenumber, which should give rise to composite, broad bands toward the low-wavenumber part of the spectra. Broadening of the component bands should normally lead to a decrease in intensity of their background, which can be observed in the B series of spectra in Figure 7.

The recorded spectra also show that oxidation and hydration occur after heating. In the spectra in Figure 7, the definite presence of a band near 1630 cm^{-1}, also reported in spectra of ludwigite by Moenke (1962), Plyusnina & Kharitonov (1963), Nekrasov & Brovkin (1966) and Franz *et al.* (1981), is completely consistent with the hydration of the samples. This band, which becomes more intense after heating, may be attributed to H–O–H bending, which implies that adsorbed H_2O was present in both the initial materials (in which the corresponding stretching mode occurs as a broad band centered at about 3360 cm^{-1}) and in heated ones. In heated samples, two intense narrow bands, which appear at about 3240 and 3560 cm^{-1}, indicate that both strongly bonded and weakly bonded hydroxyl groups coordinate with iron in hydrated compounds that result from the breakdown of magnetite.

DISCUSSION

Given the above information, one can make several statements concerning ludwigite in general. (1) Thermal, X-ray powder and infrared data on the mineral show that the hand-picked material still contain mineral impurities; it seems worthwhile, therefore, to inquire a little more carefully into the question of the vonsenite content in solid solution. (2) The strong effect of shape in the magnetic anisotropy is induced by the presence of impurities (*i.e.*, magnetite); ludwigite itself behaves superparamagnetically. (3) The unit-cell dimensions of ludwigite are not strongly related to Fe^{2+} content, because of the opposite influence of aluminum; even small contents of Al may balance the influence of increasing contents in Fe^{2+}. (4) Ludwigite is thermally inert up to 1000°C.

The mineral-composition data presented here, combined with experimental synthesis of borates, allow a reconstruction of the $T–f(O_2)$ history. As stated by Kravchuk *et al.* (1966), magnesian ludwigite needs the highest temperatures of synthesis: about 700°C for the magnesian end-member and 500–650°C for ludwigite with $X_{Fe} = 0.25$. The chemical composition of ludwigite from Ocna de Fier provides information on mineralogical constraints, implying a crystallization temperature of about 600–650°C. It compares well with the minimum temperatures of 600°C estimated from carbonate geothermometry (Marincea 1998), and thus indicates the minimum prograde temperature near the contact. In the same way, on the basis of chemical compositions and taking into account the stability fields established by Aleksandrov & Pertsev (1968) and Nitsan (1974), the oxygen fugacity during forsterite and ludwigite crystallization is inferred to have been relatively high ($fO_2 \sim 10^{-18}$ to 10^{-14} atm). The most likely source for constituents other than magnesium is the Ocna de Fier intrusive body. Initial post-skarn alteration took place at temperatures above or near 300°C, with a basic pH required by the crystallization of szaibelyite and serpentines.

ACKNOWLEDGEMENTS

Financial support for this study has been provided by the French Government, in the form of a doctoral fellowship granted to the author. The staff of Ecole Nationale Supérieure des Mines of Saint-Etienne was of invaluable help. The author is deeply indebted to Messrs. Hubert Rémy, Michel Fialin and to Mrs. Claudette Richard (Université Paris VI) for their generous assistance in carrying out the electron-microprobe analyses. Special thanks are extended to Dr. Jean Ladrière (INAN Laboratory, Université Catholique de Louvain) for performing and processing the Mössbauer spectra. Thanks are also expressed to Mrs. Gabriela Stelea (Geological Institute, Bucharest) for infrared analyses, Mr. Traian Draghiciu (Geological Institute, Bucharest) for thermal records, Mr. Jacques Moutte (Ecole Nationale Supérieure des Mines, Saint-Etienne) for ICP–AES determinations, Mrs. Jacqueline Vander Auwera-Coppens (Université de Liège) for ICP–MS measurements, and Mrs. Doina Necsulescu (PROSPECTIUNI S.A. Bucharest) for wet-chemical analyses. The quality of this contribution was improved after reviews by Drs. Nikolai N. Pertsev and Ronald Peterson. Drs. Robert F. Martin and George W. Robinson are acknowledged for editorial assistance and useful suggestions.

REFERENCES

ALEKSANDROV, S.M. (1961): Some geochemical peculiarities of the process of szaibelyitization of magnesium–iron borates. *Geokhimiya* **6**, 493-499 (in Russ.).

________ (1968): Mineralogy and diagnosis of magnesian-ferruginous borates in the ludwigite–vonsenite series. *Mineral. Syrye* **18**, 102-115 (in Russ.).

________ (1982): *Geochemistry of Boron and Tin in Magnesian Skarn Deposits*. Nauka, Moscow, Russia (in Russ.).

________, AKHMANOVA, M.V. & KARYAKIN, A.V. (1965): Investigation of borate minerals in ludwigite–vonsenite series by means of IR spectra. *Geokhimiya* **9**, 1114-1119 (in Russ.).

________ & PERTSEV, N.N. (1968): Correlation between compositions of magnesium–iron borates and minerals associated with them in magnesian skarns. *Geokhimiya* **11**, 1328-1337 (in Russ.).

Ammou-Chokroum, M. & Pianelli, A. (1970): Etude du comportement thermique de matériaux ferralitiques à l'aide d'un four monté sur diffractomètre à rayons X. *Bull. Soc. fr. Minéral. Cristallogr.* **93**, 101-113.

Appleman, D.E. & Evans, H.T., Jr. (1973): Indexing and least-squares refinement of powder diffraction data. *U.S. Geol. Surv., Comput. Contrib.* **20** (*NTIS Doc.* **PB2-16188**).

Basta, E.Z. (1957): Accurate determination of the cell dimensions of magnetite. *Mineral. Mag.* **31**, 431-442.

Bauminger, R., Cohen, S.G., Marinov, A., Ofer, S. & Segal, E. (1961): Study of the low-temperature transition in magnetite and the internal fields acting on iron nuclei in some spinel ferrites, using Mössbauer absorption. *Phys. Rev.* **122**, 1447-1450.

Benoit, P.H. (1987): Adaptation to microcomputer of the Appleman–Evans program for indexing and least-squares refinement of powder-diffraction data for unit-cell dimensions. *Am. Mineral.* **72**, 1018-1019.

Bonazzi, P. & Menchetti, S. (1989): Contribution to the crystal chemistry of the minerals of the ludwigite – vonsenite series. *Neues Jahrb. Mineral., Monatsh.*, 69-83.

Bonnin, D., Muller, S. & Calas, G. (1982): Le fer dans les kaolins. Etude par spectrométries RPE, Mössbauer, EXAFS. *Bull. Minéral.* **105**, 467-475.

Caillère, S. (1936): Contribution à l'étude des minéraux de serpentines. *Bull. Soc. fr. Minéral.* **59**, 163-326.

Capdecomme, L. (1946): Propriétés optiques nouvelles de quelques minerais de fer orthorhombiques. *Bull. Soc. fr. Minéral.* **69**, 24-41.

Cioflica, G. & Vlad, S. (1973): Contributions à la connaissance des types structuraux des pyrométasomatites laramiens de Roumanie. *Rev. Roum. Géol. Géophys. Géogr., Géol.* **17**, 3-14.

Codarcea, A., Kissling, A. & Kissling, M. (1957): Asupra ludwigitului de la Ocna de Fier. *Bul. St. Geol.-Geogr.* **3-4, II**, 515-527.

Cressey, B.A. (1979): Electron microscopy of serpentinite textures. *Can. Mineral.* **17**, 741-756.

Duval, C. & Lecomte, J. (1952): Spectres d'absorption infrarouges des ions du type BO_2^- et BO_3^{-}. *Bull. Soc. Chim. France* **19**, 101-105.

Egger, K. (1963): Zur Oxydation natürlicher Magnetite. *Schweiz. Mineral. Petrol. Mitt.*, **43**, 493-497.

Franz, G., Ackermand, D. & Koch, E. (1981): Karlite, $Mg_7(BO_3)_3(OH,Cl)_5$, a new borate mineral and associated ludwigite from the Eastern Alps. *Am. Mineral.* **66**, 872-877.

Galan, E., Liso, M.J. & La Iglesia, A. (1981): Comportamiento termico de la vonsenita. *Soc. Españ. Mineral., Volumen Extraordinario* **2**, 35-40.

Gheith, M.A. (1952): Differential thermal analysis of certain iron oxides and oxide hydrates. *Am. J. Sci.* **250**, 677-695.

Hang K'an-Tzu (1957): The fibrous ludwigite of Kuantien. *Geol. Rev.* **17**, 180-182 (in Chinese).

Hawthorne, F.C. (1988): Mössbauer spectroscopy. *In* Spectroscopic Methods in Mineralogy and Geology. *Rev. Mineral.* **18**, 255-340.

Hrouda, F. (1982): Magnetic anisotropy. *Geophys. Surv.* **5**, 37-82.

Ilinca, G. (1998): *Cristalochimia sulfosarurilor de bismut din provincia banatitica.* Ph.D. thesis, University of Bucharest, Bucharest, Romania.

Iosof, V. & Neacsu, V. (1980): Analysis of silicate rocks by atomic absorption spectrometry. *Rev. Roum. Chim.* **25**, 589-597.

Irwin, M.B. & Peterson, R.C. (1999): The crystal structure of ludwigite. *Can. Mineral.* **37**, 939-944.

Kan Xuemin, Xie Hongsen, Li Yirong & Zhang Enlin (1984): The magnetically-ordering of ludwigite and synthetic vonsenite and their Mössbauer spectra. *Geol. Rev.* **29**, 928-931 (in Chinese).

Kanishchev, A.D. & Pertsev, N.N. (1969): Kotoite and alumoludwigite mineralization in the Korotkovskoye skarn deposit (central Transbaikalia). *Geol. Rud. Mest.* **11**, 42-51 (in Russ.).

Kauffman, A.J. & Dilling, E.D. (1950): Differential thermal curves of certain hydrous and anhydrous minerals, with a description of the apparatus used. *Econ. Geol.* **45**, 222-244.

Kissling, A. (1967): *Studii mineralogice si petrografice în zona de exoskarn de la Ocna de Fier (Banat).* Academiei Ed., Bucharest, Romania.

Koch, S. (1960): Ludwigite from Ocna de Fier (Vaskö, Banat, Romania). *Acta Univ. Szeged., Mineral.-Petrogr.* **13**, 9-16.

Konev, A.A., Lebedeva, V.S., Kashaev, A.A. & Ushchapovskaya, Z.F. (1970): Azoproite, a new mineral of the ludwigite group. *Zap. Vses. Mineral. Obshchest.* **99**, 225-231 (in Russ.).

Kravchuk, T.A., Nekrasov, I.Ya. & Grigoriev, A.P. (1966): Conditions of formation for the minerals in the ludwigite–vonsenite series according to experimental data. *Zap. Vses. Mineral. Obshchest.* **95**, 272-286 (in Russ.).

Kurash, V.V., Urusov, V.S., Malysheva, T.V. & Aleksandrov, S.V. (1972): Causes of Mg–Fe ordering in the ludwigite–paigeite isomorphous series. *Geochem.* **9**, 95-101.

Larsen, E.S. (1921): The microscopic determination of the nonopaque minerals. *U. S. Geol. Surv. Bull.* **679**.

Larson, H. & Chipman, J. (1954): Activity of iron in iron–platinum solid solutions. *Acta Metall.* **2**, 1-2.

Leonard, B.F., Hildebrand, F.A. & Vlisidis, A.C. (1962): Members of the ludwigite–vonsenite series and their distinction from ilvaite. *In* Petrologic Studies. A Volume to Honor A.F. Buddington. *Geol. Soc. Am., Bull.* 523-568.

Liese, H.C. (1967): An infrared absorption analysis of magnetite. *Am. Mineral.* **52**, 1198-1205.

Mallard, E. (1887): Examen des diverses substances cristallisées. *C.R. Acad. Sci. Paris* **105**, 1260.

Malysheva, T.V., Yermakov, A.N., Aleksandrov, S.M. & Kurash, V.V. (1971): Mössbauer study of isomorphism in borates of ludwigite and vonsenite series. *In* Proc. Conf. on the Application of the Mössbauer Effect (Tihany, 1969). Akademie Kiado, Budapest, Hungary (745-750).

Mandarino, J.A. (1976): The Gladstone–Dale relationship. I. Derivation of new constants. *Can. Mineral.* **14**, 498-502.

________ (1981): The Gladstone–Dale relationship. IV. The compatibility concept and its application. *Can. Mineral.* **19**, 441-450.

Marincea, S. (1998): *Cristallochimie et propriétés physiques des borates magnésiens des skarns de la province banatitique de Roumanie.* Ph.D. thesis, Ecole Nationale Supérieure des Mines de Saint-Etienne, Saint-Etienne, France.

Maxwell, J.A. (1968): *Rock and Mineral Analysis.* Interscience Publishers, London, U.K.

Moenke, H. (1962): *Mineralspektren.* Academie Verlag, Berlin, Germany.

Mokeyeva, V.I. (1968): Refinement of the structure of ludwigite $(Mg_{1.85}Fe^{2+}_{0.15})(Fe^{3+}_{0.60}Al_{0.40})BO_3O_2$ and the distributions of Mg^{2+} and Fe^{2+} in cation sites. *Geokhimiya* **8**, 975-979 (in Russ.).

________ & Aleksandrov, S.M. (1969): Distribution of magnesium and iron in the structure of borates in the ludwigite–vonsenite series. *Geokhimiya* **4**, 428-435 (in Russ.).

Murad, E. & Schwertmann, U. (1980): The Mössbauer spectrum of ferrihydrite and its relations to those of other iron oxides. *Am. Mineral.* **65**, 1044-1049.

Nekrasov, I.Ya. & Brovkin, A.A. (1966): The influence of the compositional variations of the minerals in ludwigite – vonsenite series on the configuration of their infrared spectra. *Roentgenogr. Min. Syrya* **5**, 27-32 (in Russ.).

Nicolescu, S. (1998): *Skarn genesis at Ocna de Fier - Dognecea, South-West Romania.* Ph.D. thesis, University of Göteborg, Sweden.

Nitsan, U. (1974): Stability field of olivine with respect to oxidation and reduction. *J. Geophys. Res.* **79**, 706-711.

Palache, C., Berman, H. & Frondel, C. (1951): *Dana's System of Mineralogy* (seventh ed.) **II**. John Wiley and Sons, New York, N.Y.

Pertsev, N.N. (1991): Magnesian skarns. *In* Skarns.Their Genesis and Metallogeny (A. Barto-Kyriakidis, ed.). Theophrastus Publications, Athens, Greece (299-324).

________ & Aleksandrov, S.M. (1964): Ludwigite with a high content of alumina. *Zap. Vses. Mineral. Obshchest.* **93**, 13-20 (in Russ.).

Plyusnina, I.I. & Kharitonov, Yu.A. (1963): Crystallochemical properties and infrared absorption spectra of borates and borosilicates. *Zh. Strukt. Khim.* **4**, 555-568 (in Russ.).

Pouchou, J.-L. & Pichoir, F. (1985): "PAP" $\phi(\rho z)$ procedure for improved quantitative microanalysis. *In* Microbeam Analysis (J.T. Armstrong, ed.). San Francisco Press, San Francisco, California (104-106).

Russo-Sandulescu, D., Berza, T., Bratosin, I., Vlad, C. & Ianc, R. (1986): Petrological study of banatites in the Ocna de Fier – Dognecea zone (Banat). *D. S. Inst. Geol. Geofiz.* **64**, 111-119.

Schaller, W. (1911): Ludwigit von Montana, U.S.A. *Z. Kristallogr.* **48**, 25-29.

________ & Vlisidis, A.C. (1961): The composition of aluminian ludwigite from Crestmore, California. *Am. Mineral.* **46**, 335-339.

Schwab, R.G. & Küstner, D. (1977): Präzisiongitterkonstantenbestimmung zur Festlegung röntgenographischer Bestimmungskurven für synthetische Olivine der Mischkristallreihe Forsterit – Fayalit. *Neues Jahrb. Mineral., Monatsh.*, 205-215.

Schmidt, E.R. & Vermaas, F.H.S. (1955): Differential thermal analysis and cell dimensions of some natural magnetites. *Am. Mineral.* **40**, 422-431.

Shabynin, L.I. (1955): Ascharite and other borates in magnetite ores of contact-metasomatic deposits. *Dokl. Akad. Nauk. S.S.S.R.* **101**, 937-940 (in Russ.).

Shannon, R.D. & Prewitt, C.T. (1969): Effective ionic radii in oxides and fluorides. *Acta Crystallogr.* **B25**, 925-946.

Shinno, I. & Maeda, I. (1989): Mössbauer spectra of diopside containing 4- and 6-coordinated ferric irons at 78 K and 4.2 K. *Mineral. J. (Japan)* **14**, 191-197.

Smothers, W.J. & Chiang, Y. (1966): *Handbook of Differential Thermal Analysis.* Chemical Publishing Company Inc., New York, N.Y.

Steele, W.C. & Decius, J.C. (1956): Infrared absorption of lanthanum, scandium and indium borate and the force constants of borate ion. *J. Chem. Phys.* **25**, 1184-1188.

STRONA, P.A. (1964): Reflectivity measurements of ore minerals in polished sections. *Zap. Vses. Mineral. Obshchest.* **93**, 69-72 (in Russ.).

SWINNEA, J.S. & STEINFINK, H. (1983): Crystal structure and Mössbauer spectrum of vonsenite, 2FeO•FeBO$_3$. *Am. Mineral.* **68**, 827-832.

TAKÉUCHI, Y., WATANABE, T. & ITO, T. (1950): The crystal structures of warwickite, ludwigite and pinakiolite. *Acta Crystallogr.* **3**, 98-107.

TILLEY, C.E. (1951): The zoned contact-skarns of the Broadford area, Skye: a study of boron–fluorine metasomatism in dolomite. *Mineral. Mag.* **29**, 621-666.

TODOR, D.N. (1972): *Analiza termica a mineralelor.* Tehnica Ed., Bucharest, Romania.

TRÖGER, W.E. (1969): *Optische Bestimmung der gesteinbildenden Minerale.* E. Schweizerbart'sche Ed., Stuttgart, Germany.

TSCHERMAK, G. (1874): Ludwigit, ein neues Mineral aus dem Banate. *Jahrb. der Kaiserlich-königlichen Geol. Reichsanstalt* (*Wien*) **XXIV**, 59-66.

UYEDA, S., FULLER, M.D., BELSHÉ, J.C. & GIRDLER, R.W. (1963): Anisotropy of magnetic susceptibility of rocks and minerals. *J. Geophys. Res.* **68**, 279-291.

UYTENBOGAARDT, W. & BURKE, E.A.J. (1971): *Tables for Microscopic Identification of Ore Minerals* (second ed.). Elsevier, Amsterdam, The Netherlands.

VLISIDIS, A.C. & SCHALLER, W.T. (1974): The identity of paigeite with vonsenite and chemical analyses of vonsenite, ludwigite and hulsite. *Neues Jahrb. Mineral., Monatsh.*, 95-105.

VON COTTA, B. (1864): *Erzlagerstätten im Banat und in Serbien.* W. Braumüller Ed., Wien, Austria.

WATANABE, T. (1953): Suanite, a new magnesium borate from Hol Kol, Suan, North Korea. *Mineral. J.* (*Japan*) **1**, 54-62.

WHITTAKER, E.J.W. & WICKS, F.J. (1970): Chemical differences among the serpentine "polymorphs": a discussion. *Am. Mineral.* **55**, 1025-1047.

________ & ZUSSMAN, J. (1956): The characterization of serpentine minerals by X-ray diffraction. *Mineral. Mag.* **31**, 107-126.

WICKS, F.J. & WHITTAKER, E.J.W. (1977): Serpentine textures and serpentinization. *Can. Mineral.* **15**, 459-488.

________ & ZUSSMAN, J. (1975): Microbeam X-ray diffraction patterns of the serpentine minerals. *Can. Mineral.* **13**, 244-258.

XIE HONGSEN, PENG WENSHI, ZHANG YUEMING, XU HUIGANG & LAI ZHAOSHENG (1985): A study of the synthetic ludwigite series. *Acta Mineral. Sinica* **5**, 102-108 (in Chinese, English abstr.).

YERMAKOV, A.N., ALEKSANDROV, S.M., KURASH, V.V. & MALYSHEVA, T.V. (1969): Examination of isomorphism of magnesium and iron in the ludwigite–vonsenite borate series by Mössbauer spectroscopy. *Geochem.* **6**, 956-962.

Received November 28, 1998, revised manuscript accepted September 25, 1999.